

30th IAEA Fusion Energy Conference (IAEA-FEC)



Construction Progress of Chinese First Quasi-axisymmetric Stellarator (CFQS)

Preliminary Results in the CFQS-Test Device

and

Y. Xu¹, <u>H. F. Liu¹</u>, J. Cheng¹, X. Q. Wang¹, J. Huang¹, H. Liu¹, X. Zhang¹, J. F. Shen¹, J. Hu¹, H. Lan¹, Y. C. Li¹, W. Li¹, W. M. Xuan¹, C. J. Tang^{1,3}, A. Shimizu^{2,5}, M. Isobe^{2,5}, S. Okamura², S. Kinoshita², K. Ogawa^{2,5}, R. Seki^{2,5}, Y. Yoshimura^{2,5}, M. Nakata^{2,5}, W. A. Cooper^{2,6}, H. Takahashi^{2,5}, T. Oishi^{2,5}, M. Osakabe^{2,5}, T. Murase², S. Nakagawa², H. Tanoue², H. Hayashi², S. Kobayashi², D. P. Yin⁴, J. F. Zhao⁴, A. Z. Wang⁴, L. Zhong⁴, X. N. Wu⁴ and CFQS team

¹ Institute of Fusion Science, School of Physical Science and Technology, Southwest Jiaotong University, Chengdu 610031, China

² National Institute for Fusion Science, National Institutes of Natural Sciences, Toki 509-5292, Japan

³ Physics Department, Sichuan University, Chengdu 610041, China

⁴ Hefei Keye Electro Physical Equipment Manufacturing Co., Ltd, Hefei, 230000, China

⁵ SOKENDAI (The Graduate University for Advanced Studies), Toki 509-5292, Japan

⁶ Ecole Polytechnique Fédérale de Lausanne, Swiss Plasma Center, Station 13, CH-1015 Lausanne, Switzerland



Outline



- Physical characteristics of CFQS
- Construction progress of CFQS
- Scientific achievements on CFQS-T
- Summary

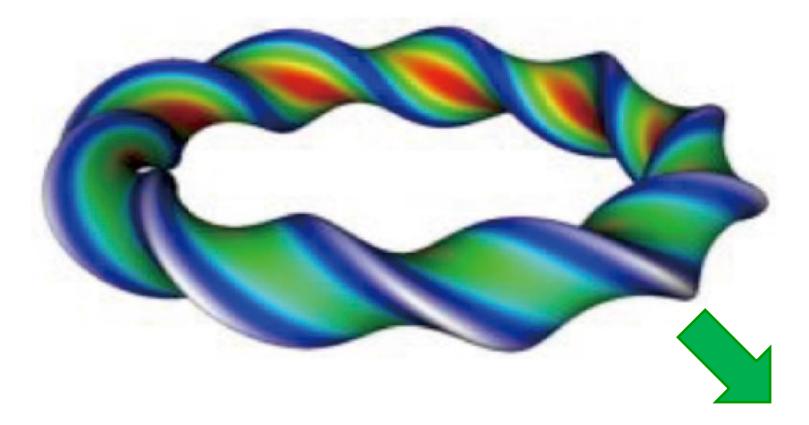
Basic idea of a QA device

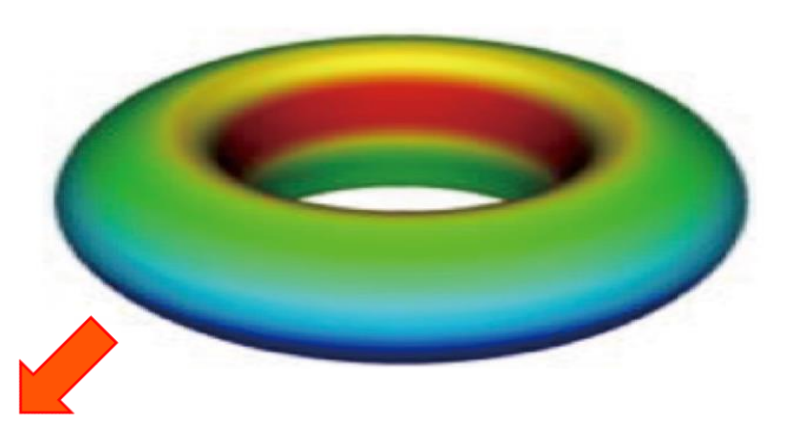
Stellarator

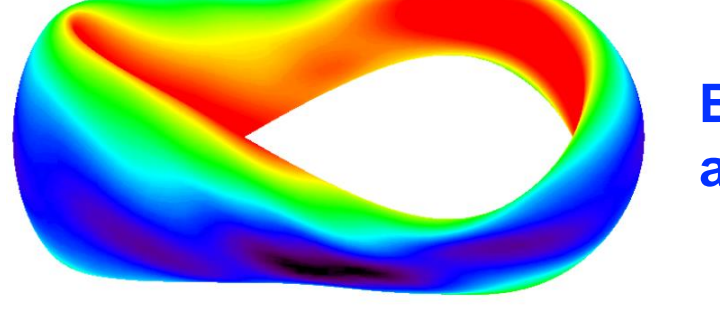
- No inductive plasma current
 - → Steady-state operation capability
- Large neoclassical transport by ripple diffusion



- Requiring plasma current
 - → Major disruption, pulse operation
- Reduced neoclassical transport and good particle orbit by axisymmetry







Both advantages are combined

Quasi-axisymmetry

Optimization strategy of CFQS

The Chinese First Quasi-axisymmetric Stellarator (CFQS):

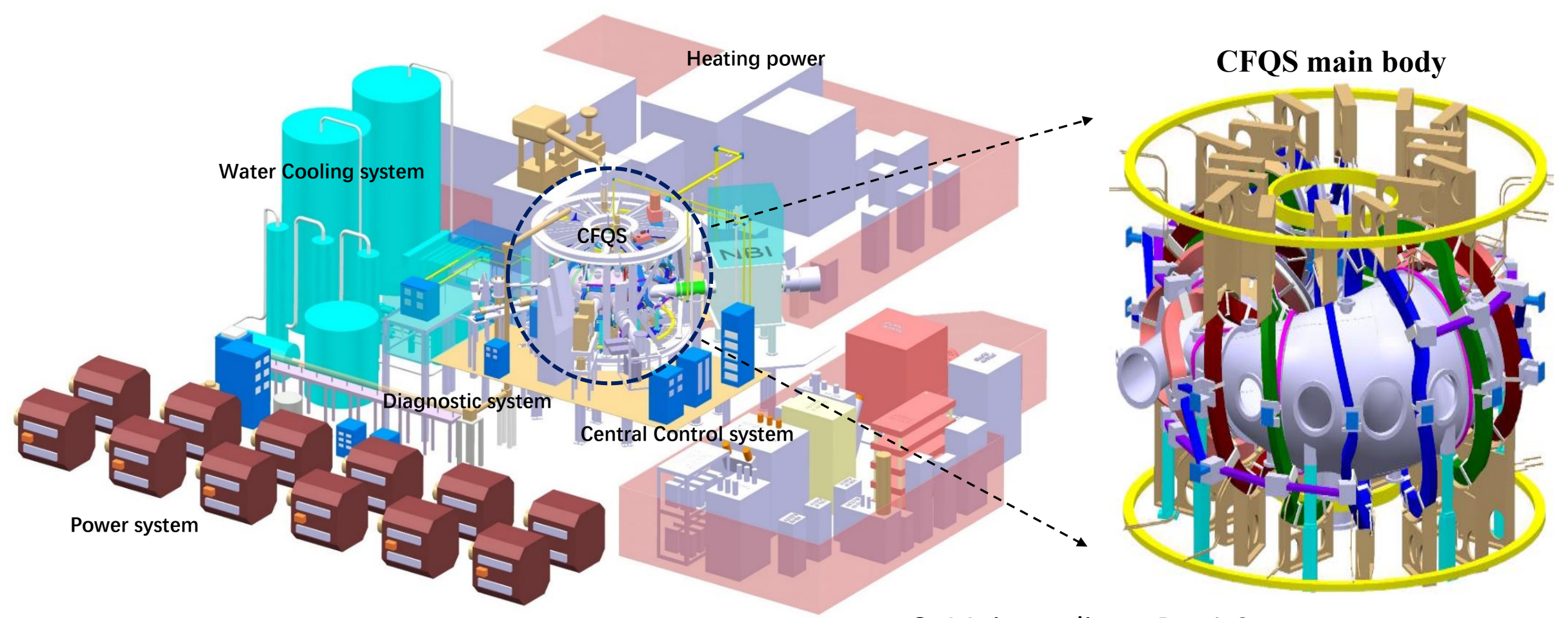
- Jointly designed by SWJTU (China) and NIFS (Japan), and constructed by SWJTU.
- Main purpose is to verify the advantage of quasi-axisymmetric stellarator in reducing neoclassical transport for the first time in the world.

Major properties	Perspective improvement
Quasi-axisymmetric configuration	Reducing neoclassical transport
Magnetic well	Good MHD stability
Low aspect ratio	Large plasma volume
Low toroidal viscosity (high toroidal rotation)	Suppressing anomalous transport by sheared flows

Y. Xu, H. F. Liu, A. Shimizu, M. Isobe, S. Okamura, S. Kinoshita et al., 27th IAEA(2018), EX/p5-23.

M. Isobe et al., 45th EPS Conference on Plasma Physics, P2.1043 (2018).

Schematic of the CFQS device



J. Cheng et al., PPCF 67 (2025) 105011 Y. Xu, Stellarator News, 170 (2020)

H.F. Liu et al., PFR 13 (2018) 3405067

A. Shimizu et al., PFR 13 (2018) 3403123

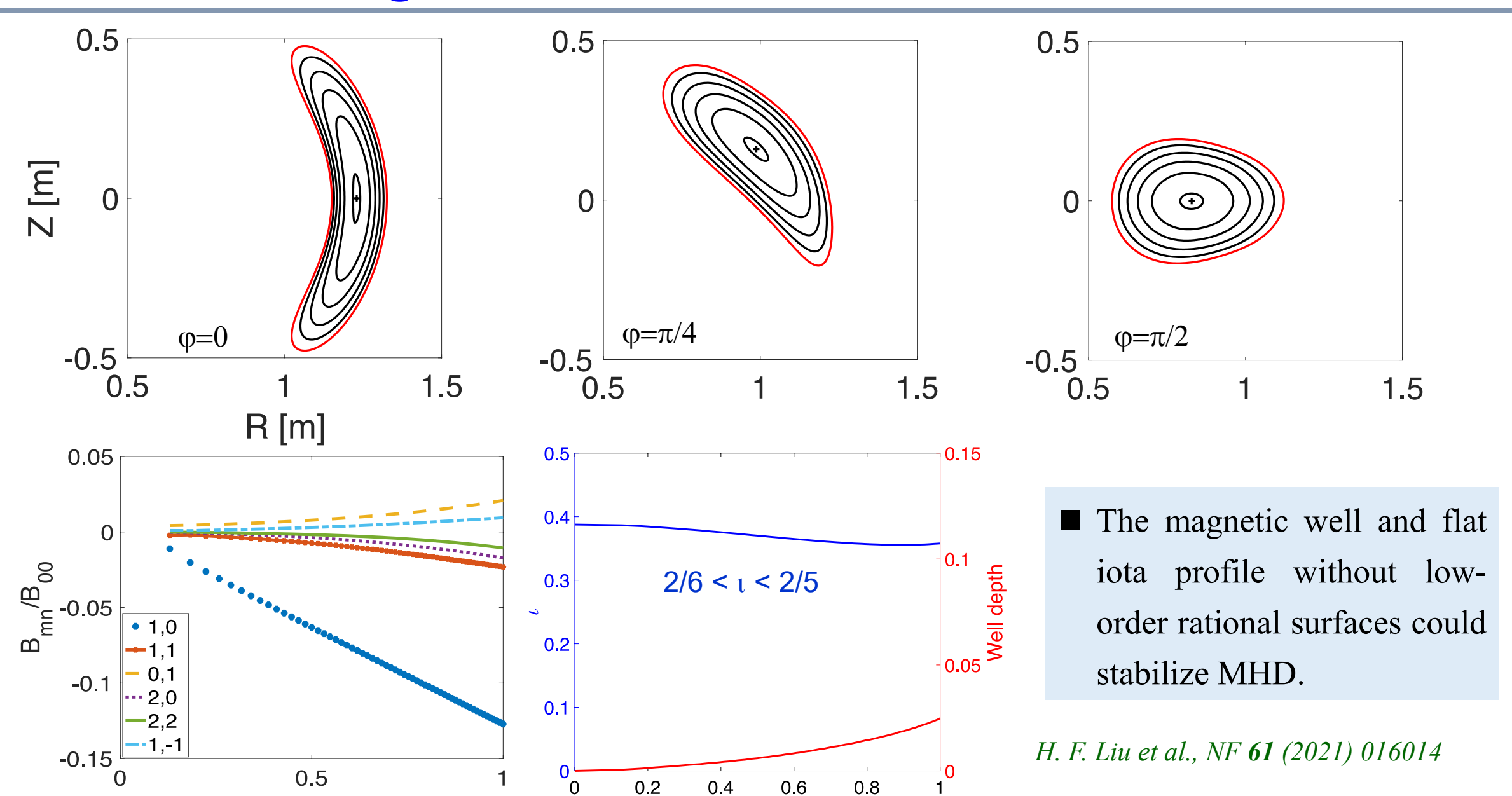
● Major radius: R = 1.0 m,

• Averaged minor radius: $\langle a \rangle \approx 0.25 \text{ m}$

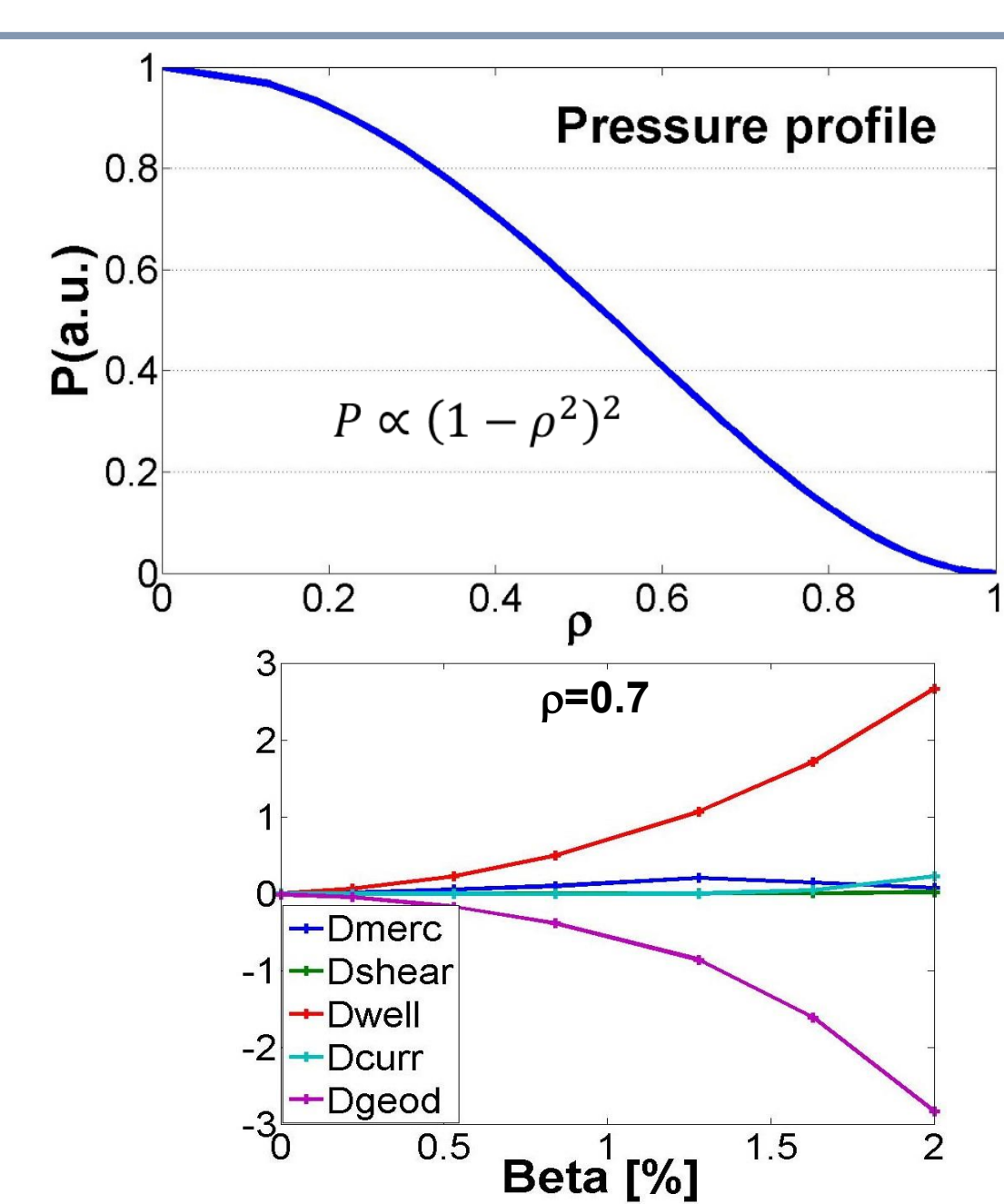
• Magnetic field: $B_t \approx 1.0 \text{ T}$

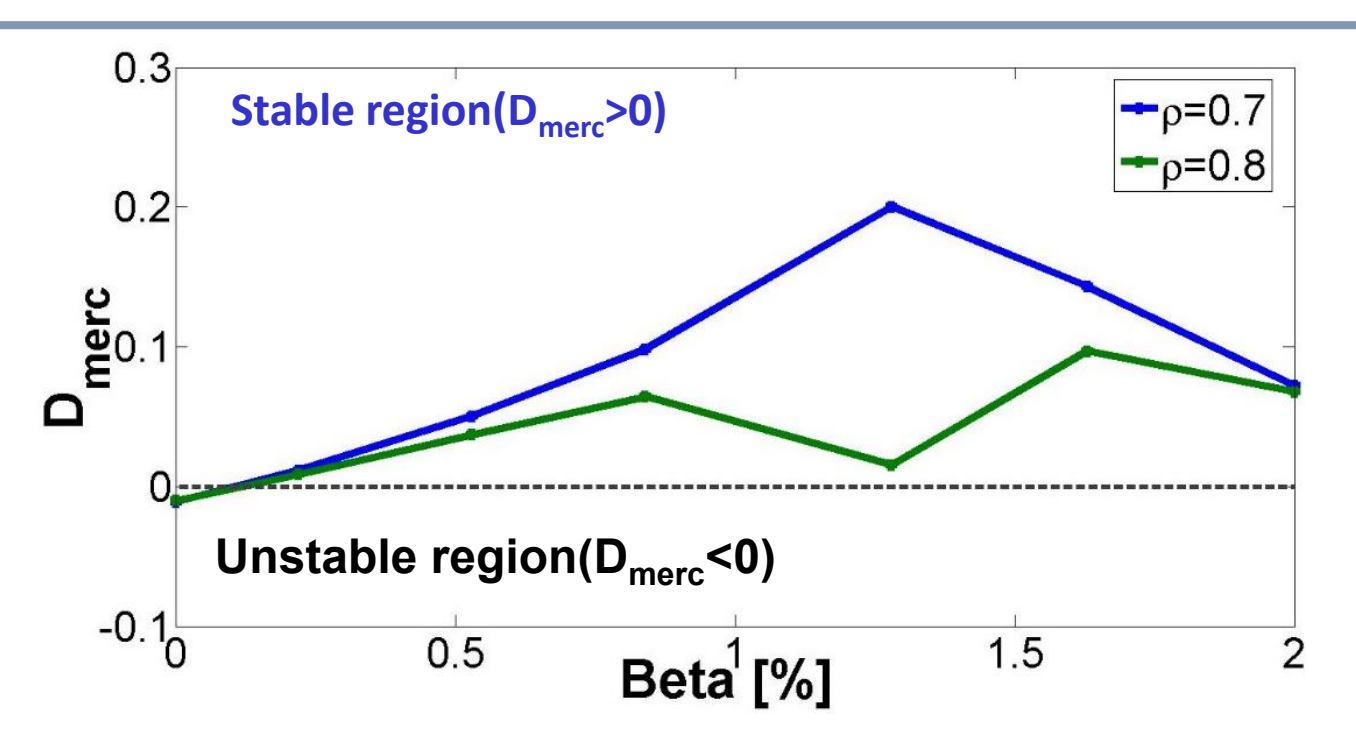
• Toroidal periodic number: $N_p = 2$

Configuration characteristics of CFQS



Mercier instability in CFQS

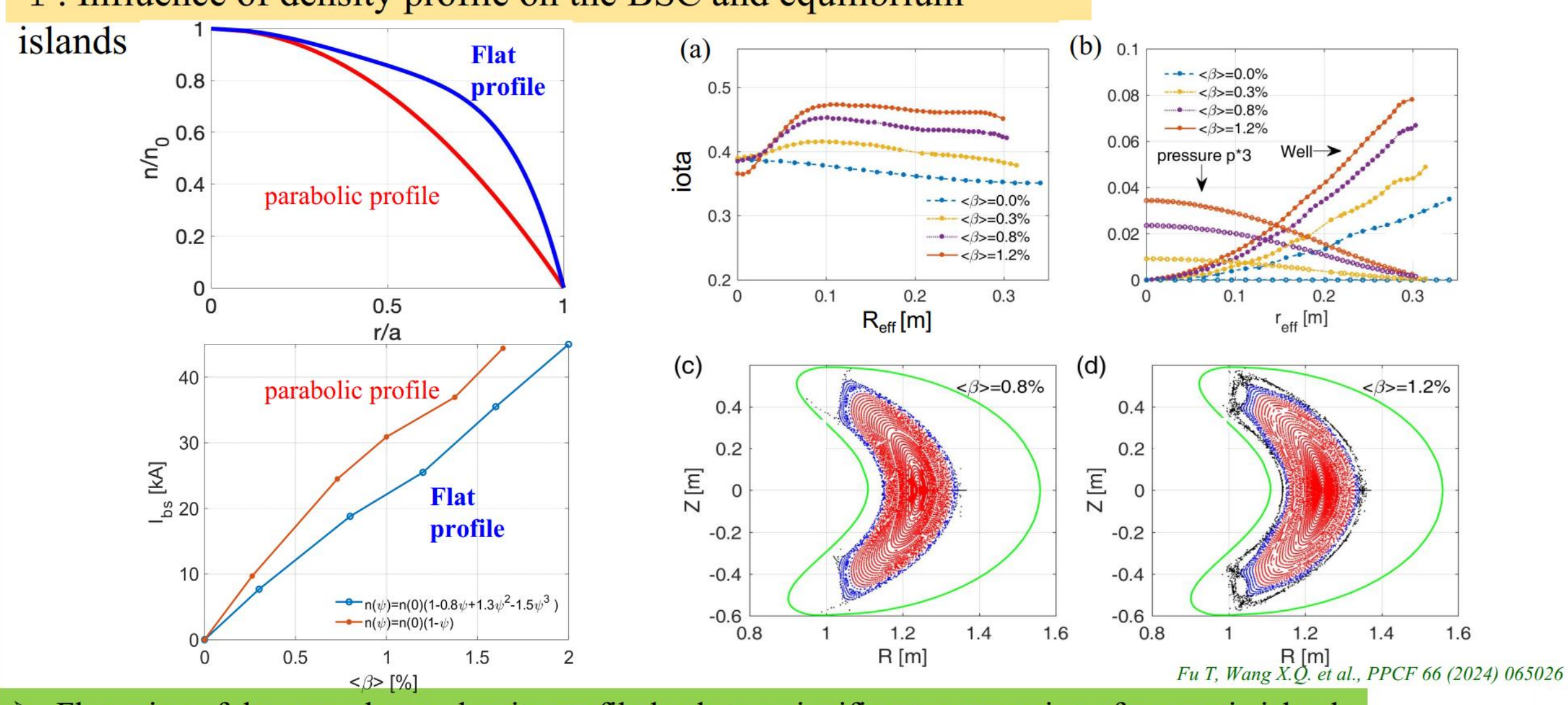




- ❖ The Mercier stability criterion is expressed as: $D_{merc} = D_{shear} + D_{well} + D_{curr} + D_{geod} > 0;$
- ❖ Up to beta=2%, the interchange mode is stable.

Suppression of islands by density control

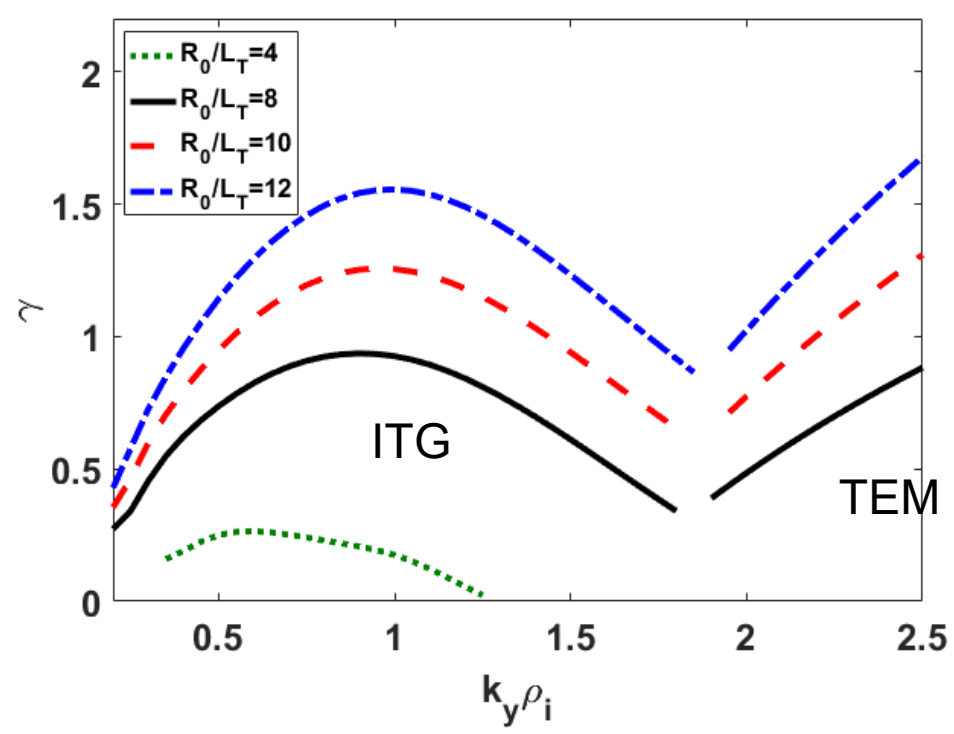
I . Influence of density profile on the BSC and equilibrium



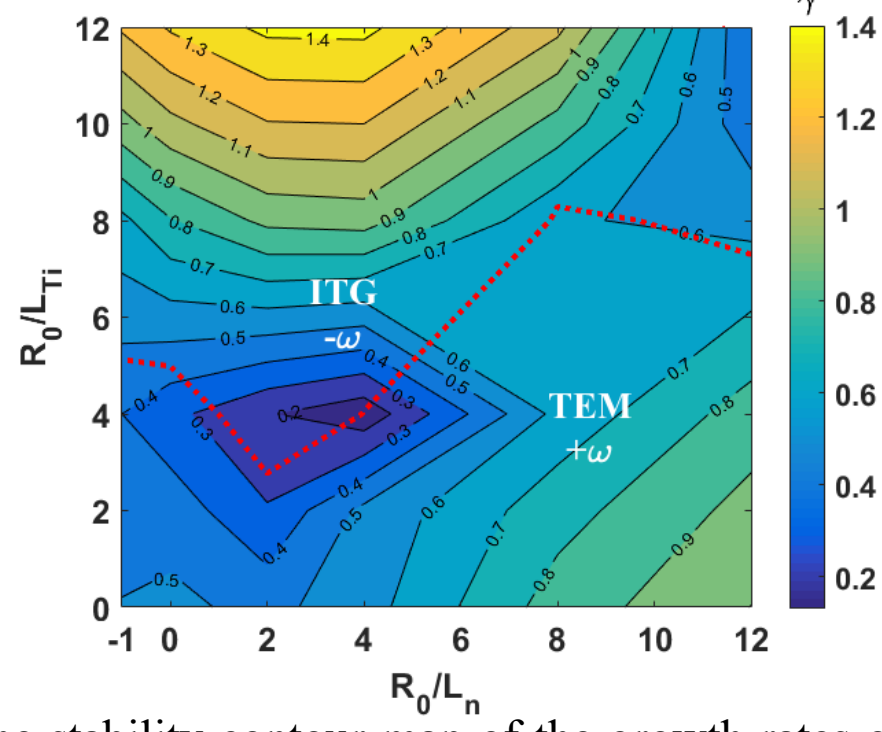
> Flattening of the core plasma density profile leads to a significant suppression of magnetic islands.

Hybrid ITG-TEM simulations in CFQS

J. Huang et. al., PoP 29 (2022) 052505



The growth rates of the hybrid ITG-TEM modes vs. $k_y \rho_i$ for various R_0/L_T at $R_0/L_n = 2$.



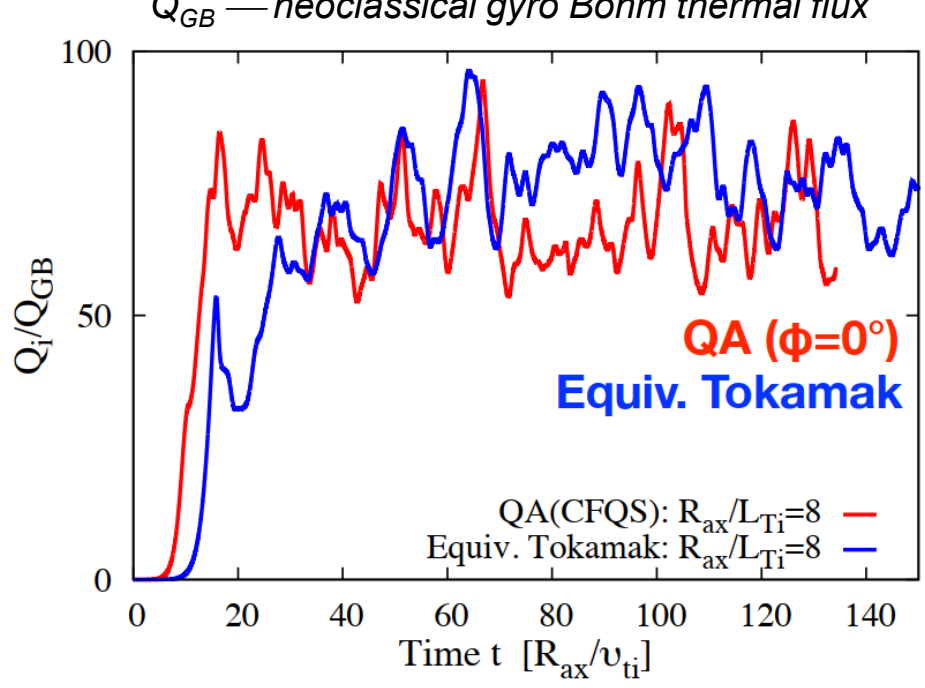
The stability contour map of the growth rates of the electrostatic hybrid ITG-TEM modes vs. R_0/L_n and R_0/L_{T_i} for $R_0/L_{T_e} = 8$ and $k_y \rho_i = 1$.

- In the low $k_y \rho_i$ region, the dominant mode is ITG and in the high $k_y \rho_i$ region, the dominant mode is TEM.
- lackloais The TEM is the dominant mode when R_0/L_{T_i} is small. As R_0/L_{T_i} increases, the dominant mode is transited into ITG mode. It is found that a stability-valley-like structure appears in the stability map for the ion-scale modes.

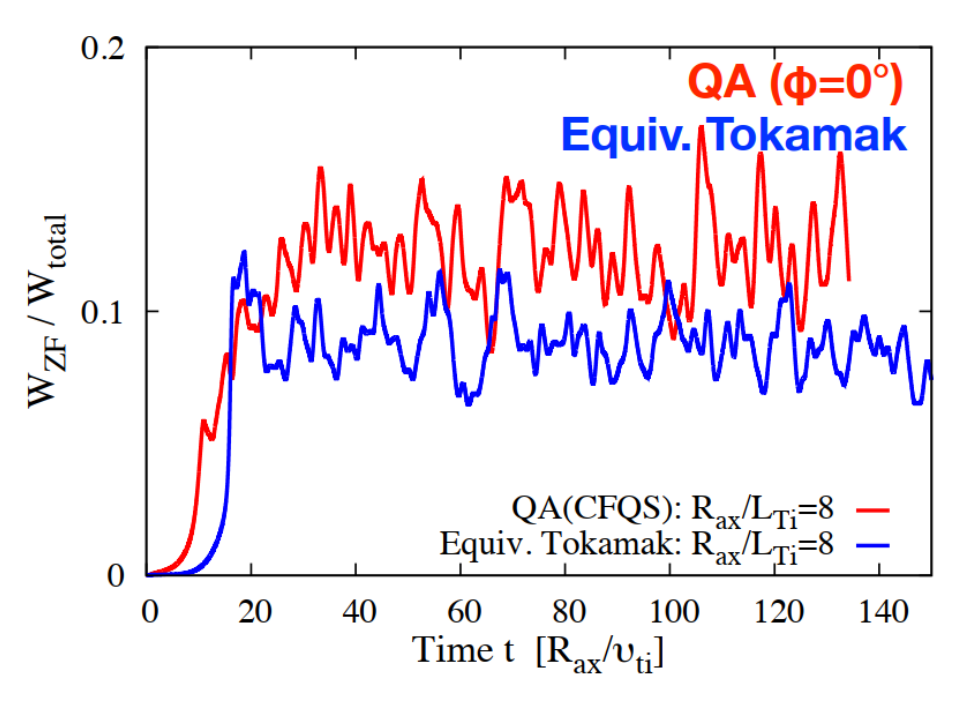
Nonlinear ITG turbulence simulations in CFQS



Q_i — turbulent ion thermal flux Q_{GB} — neoclassical gyro Bohm thermal flux



Zonal-flow

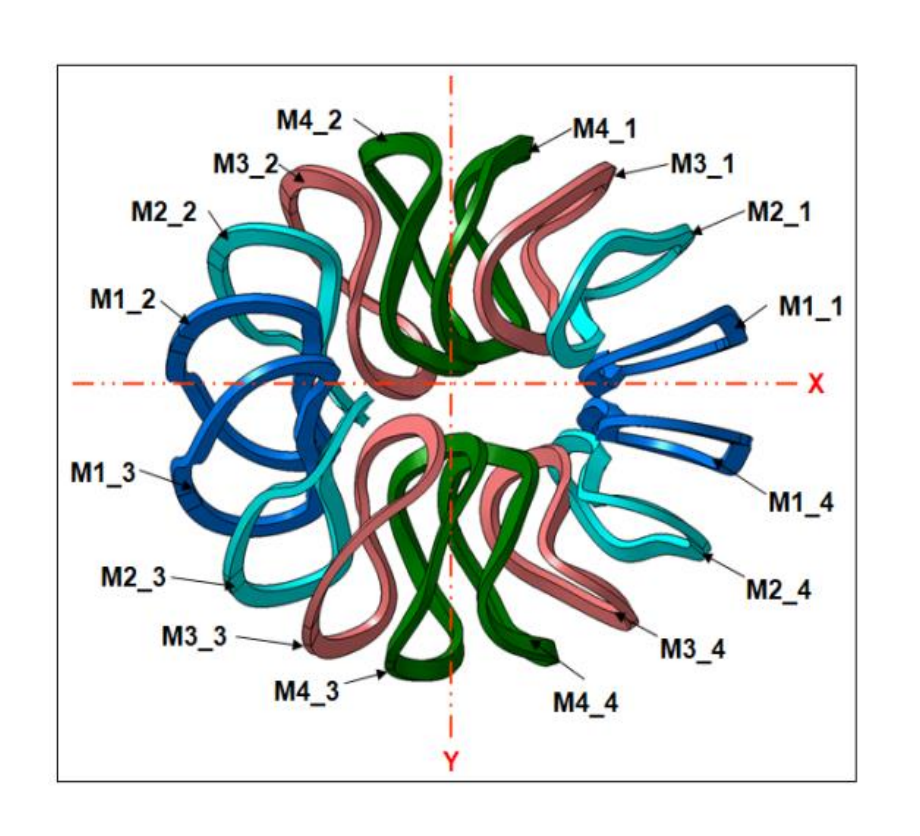


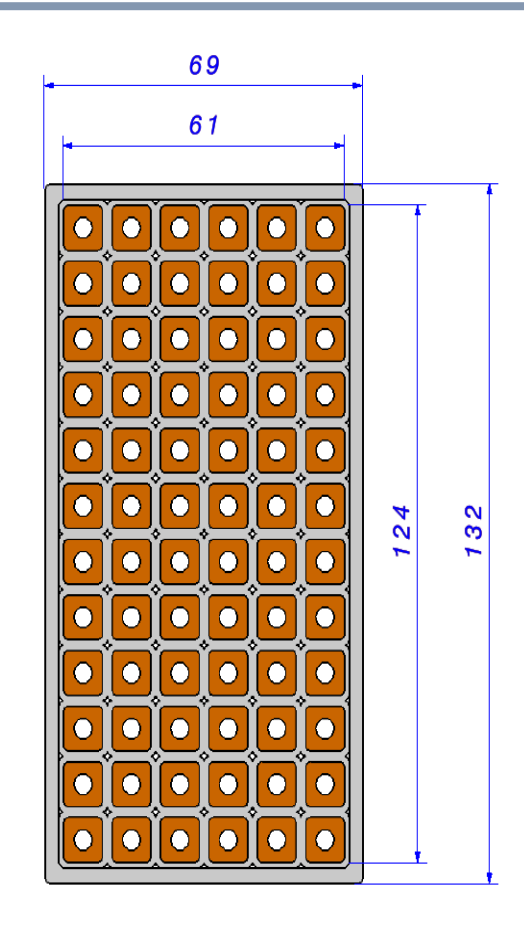
Equivalent circular tokamak with the same q, s and A_p .

M. Nakata et al., 27th ITC(2018), O-1

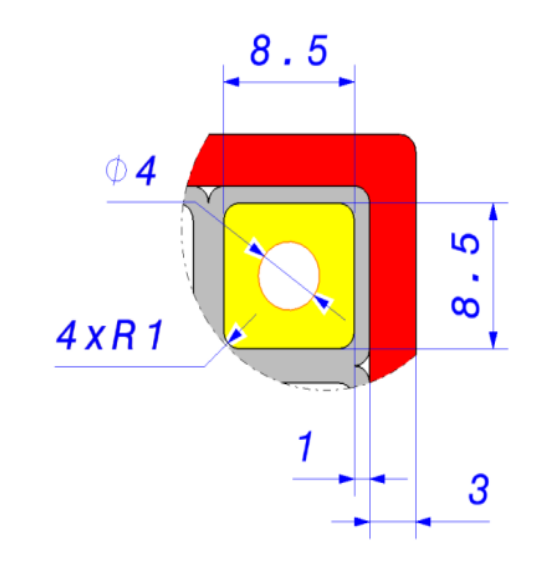
- The nonlinear turbulent heat flux in CFQS is comparable or less than that in the Equivalent Tokamak.
- ♦ Enhanced zonal-flow generation is found in CFQS, indicating remarkable impacts of the quasiaxisymmetry on the nonlinear interactions.

Modular coils (copper conducts) of CFQS



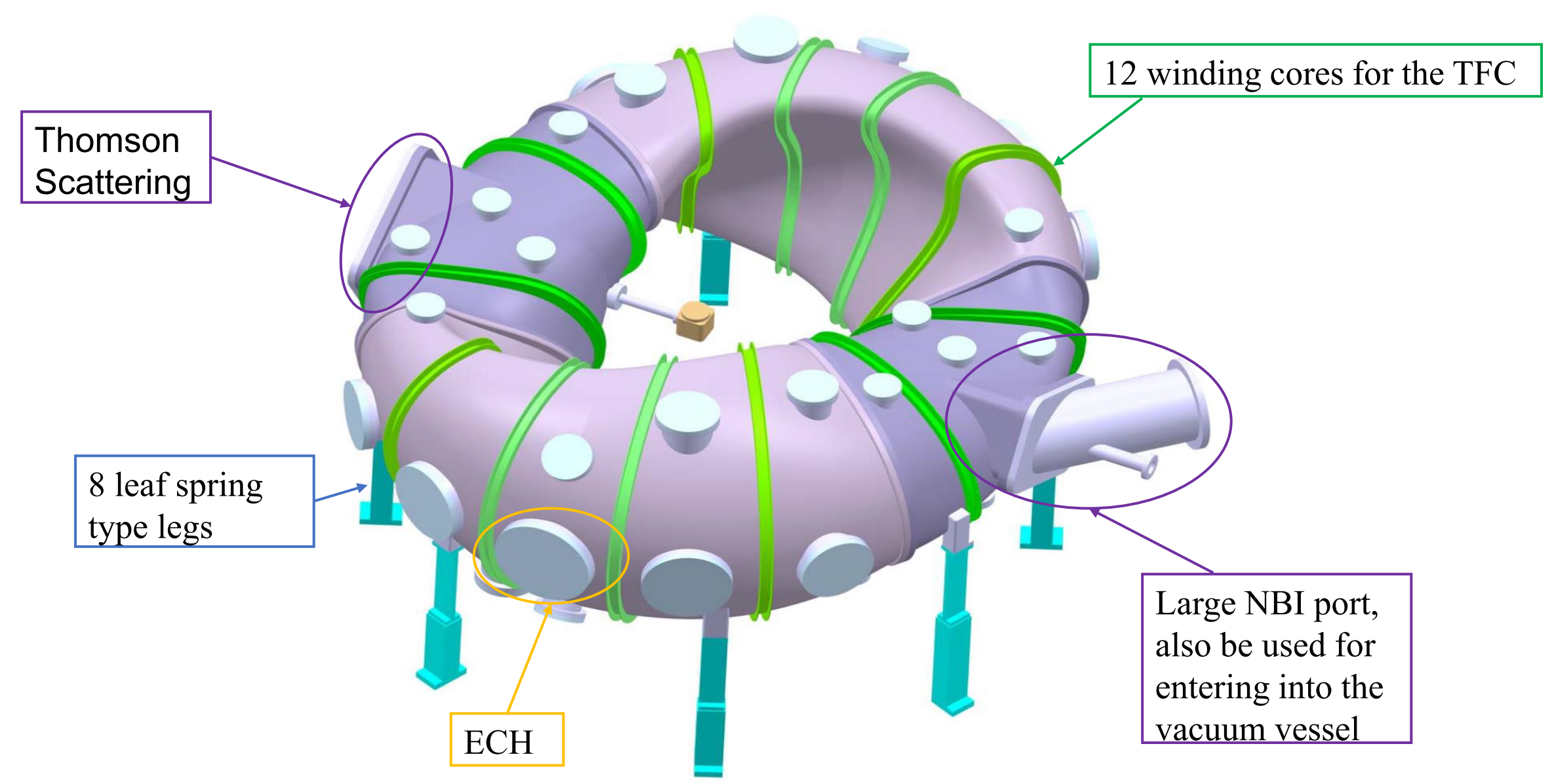


4.34 kA * 72 = 312.5 kA



- > The modular coil system consists of four pairs of coils (M1, M2, M3, M4) with four different shapes;
- > The area of cross section for each coil is 132mm × 69mm;
- > There are 6x12 hollow copper conductors in each coil; (4.34 kA * 72 = 312.5 kA)
- > Copper conductor (8.5 mmx 8.5 mm) with a hollow for the water cooling channel.

Vacuum vessel design of CFQS



CFQS research plan

♦ 0.1 T operation

 \triangleright ECH: $P \sim 20$ kW, f = 2.45GHz

for testing of accuracy of a QA magnetic topology

♦ 1.0 T operation

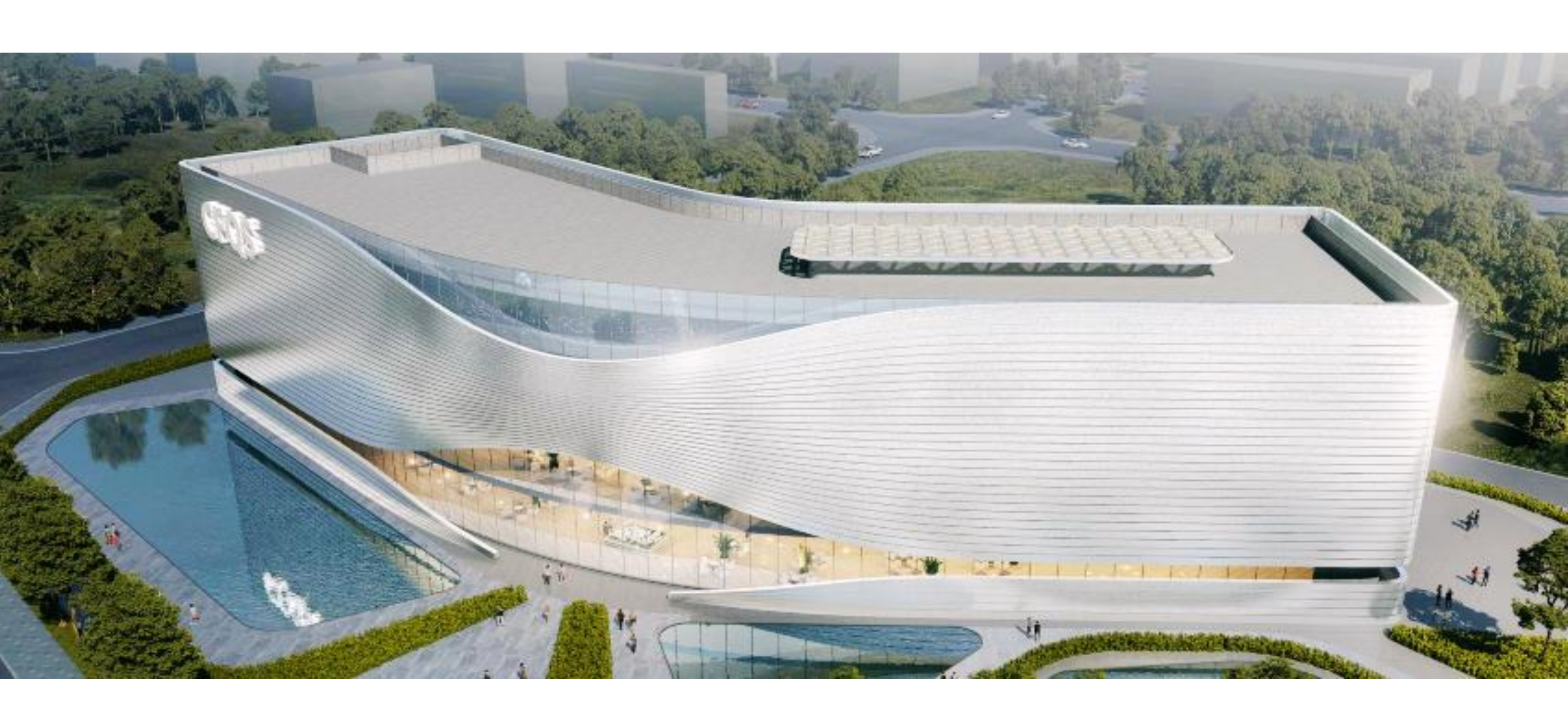
- > ECH: P ~ 450 kW, f = 54.5 GHz
- ➤ NBI (H): P ~ 1.0 MW, E < 40 keV</p>

Delve into plasma properties with high plasma parameters

Laboratory of CFQS-T in JiuLi campus



Schematics in TianFu New Zone





Outline



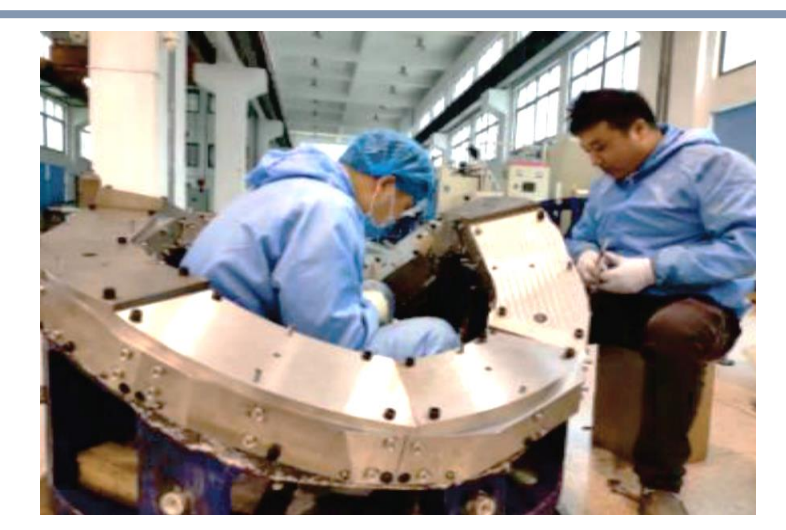
- Physical characteristics of CFQS
- Construction progress of CFQS
- Scientific achievements on CFQS-T
- Summary

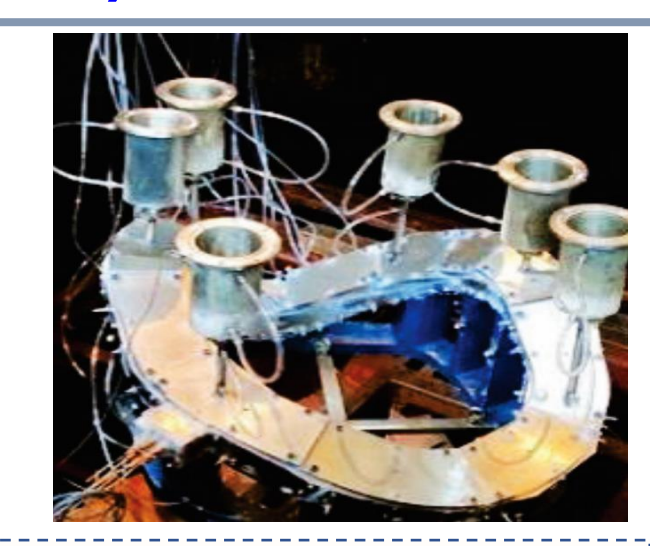
Fabrication of mock up coil (MC4)

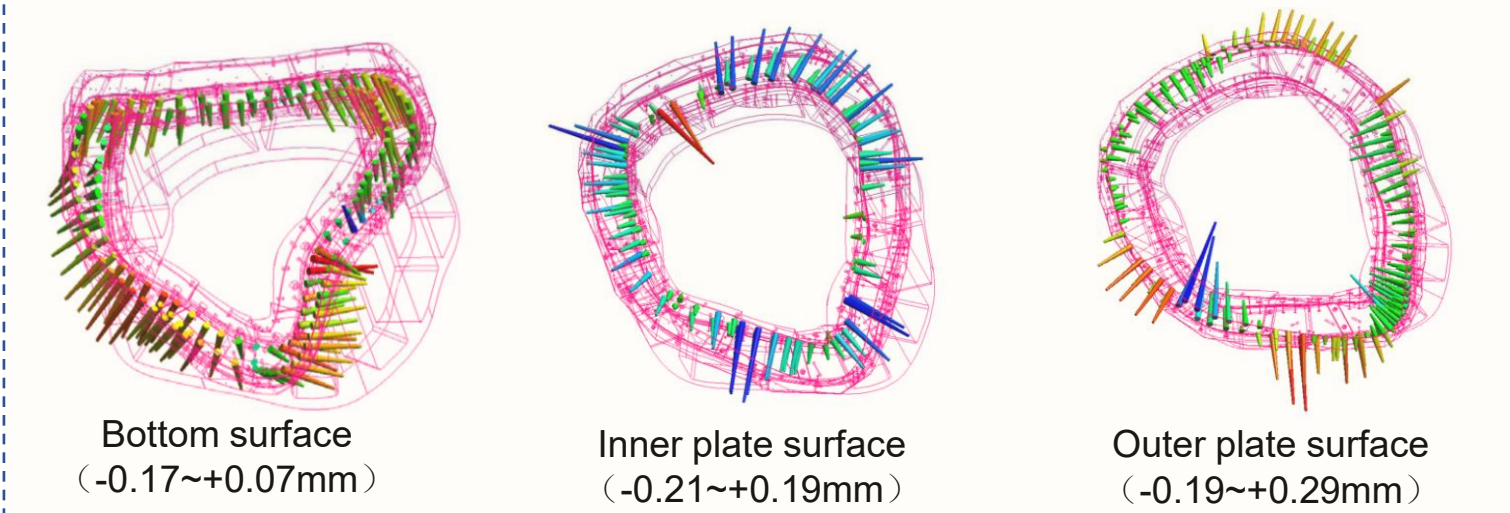




finished mockup coil 4

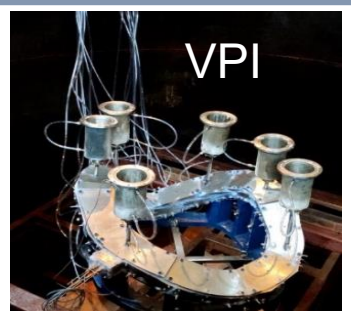




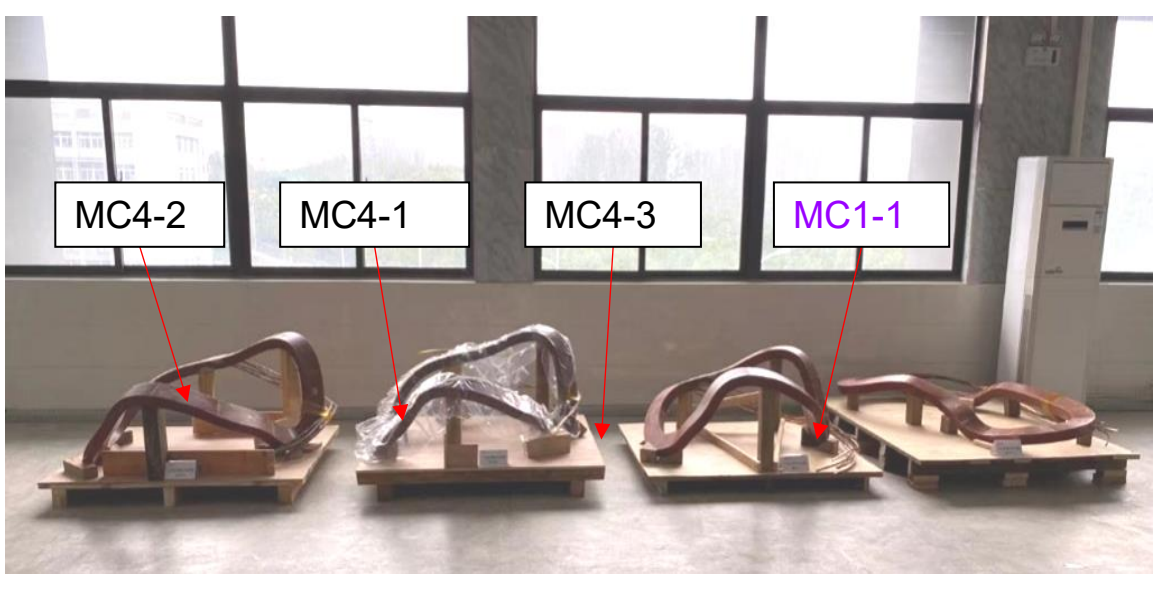


- The mockup coil: winding, modify mould and VPI;
- Dimension measurement by laser tracker, meet the design;
- Start to manufacture the other MC coils.

Manufactured modular coils (4 types)



- Totally 16 modular coils has been winded (4-MC1, 4-MC2, 4-MC3, 4-MC4);
- Compared with 3D model, deviation is within 1.2 mm, which is acceptable range;
- Two times VPI of 16 coils has been finished at the end of March, 2024;
- The insulation and heat test has been finished at the end of May, 2024.















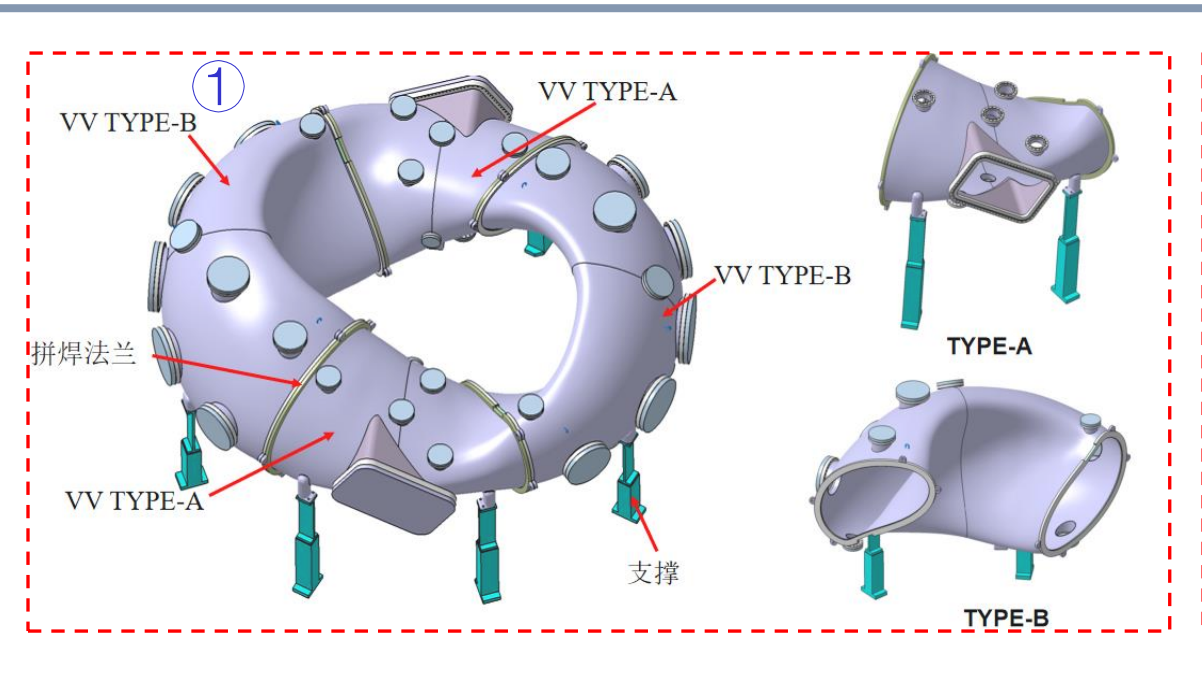


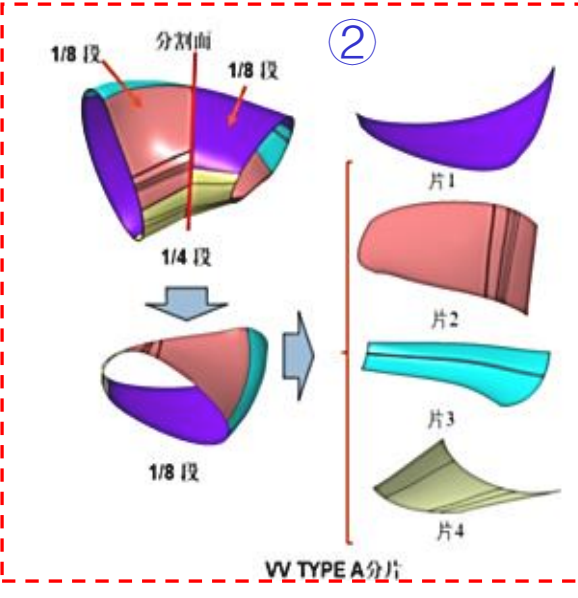
MC1-2

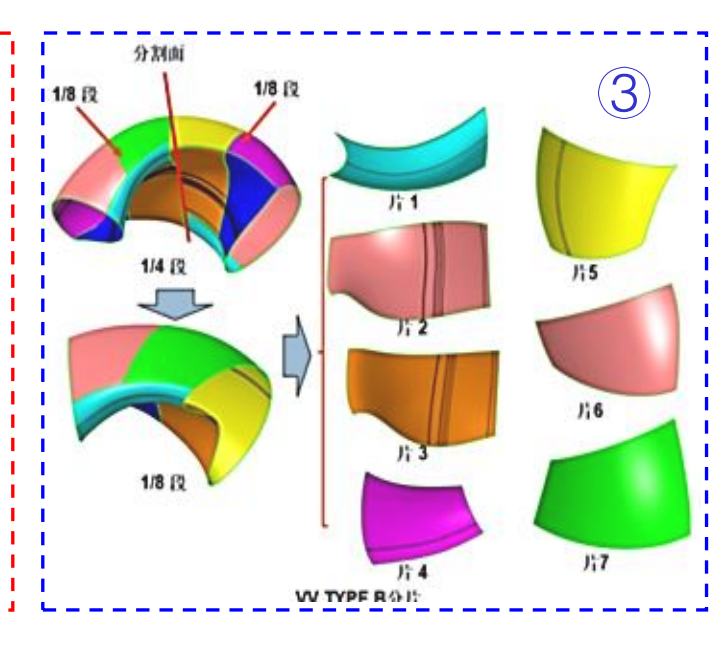
MC1-3

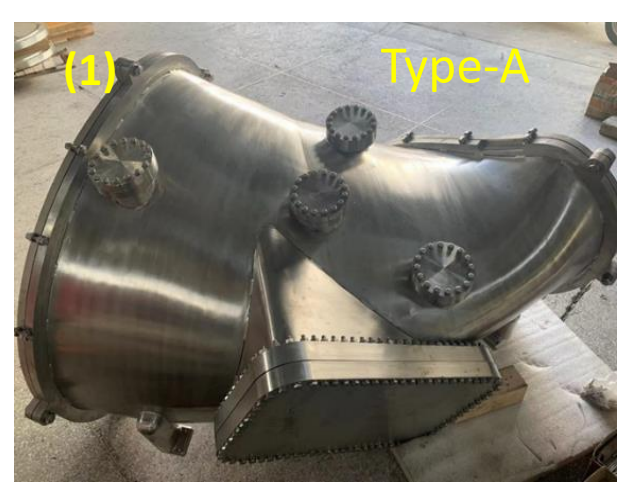
MC3-1

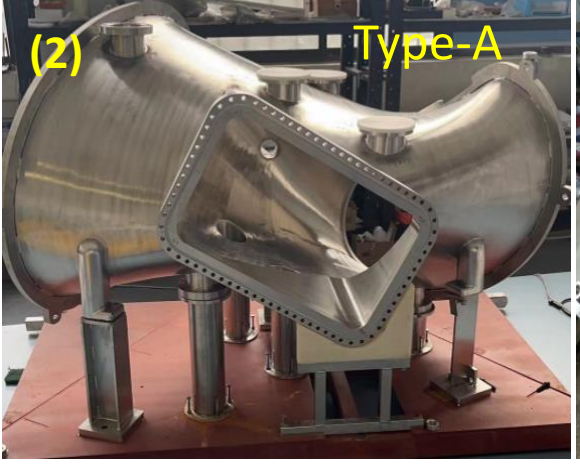
Manufacture of Vacuum Vessel











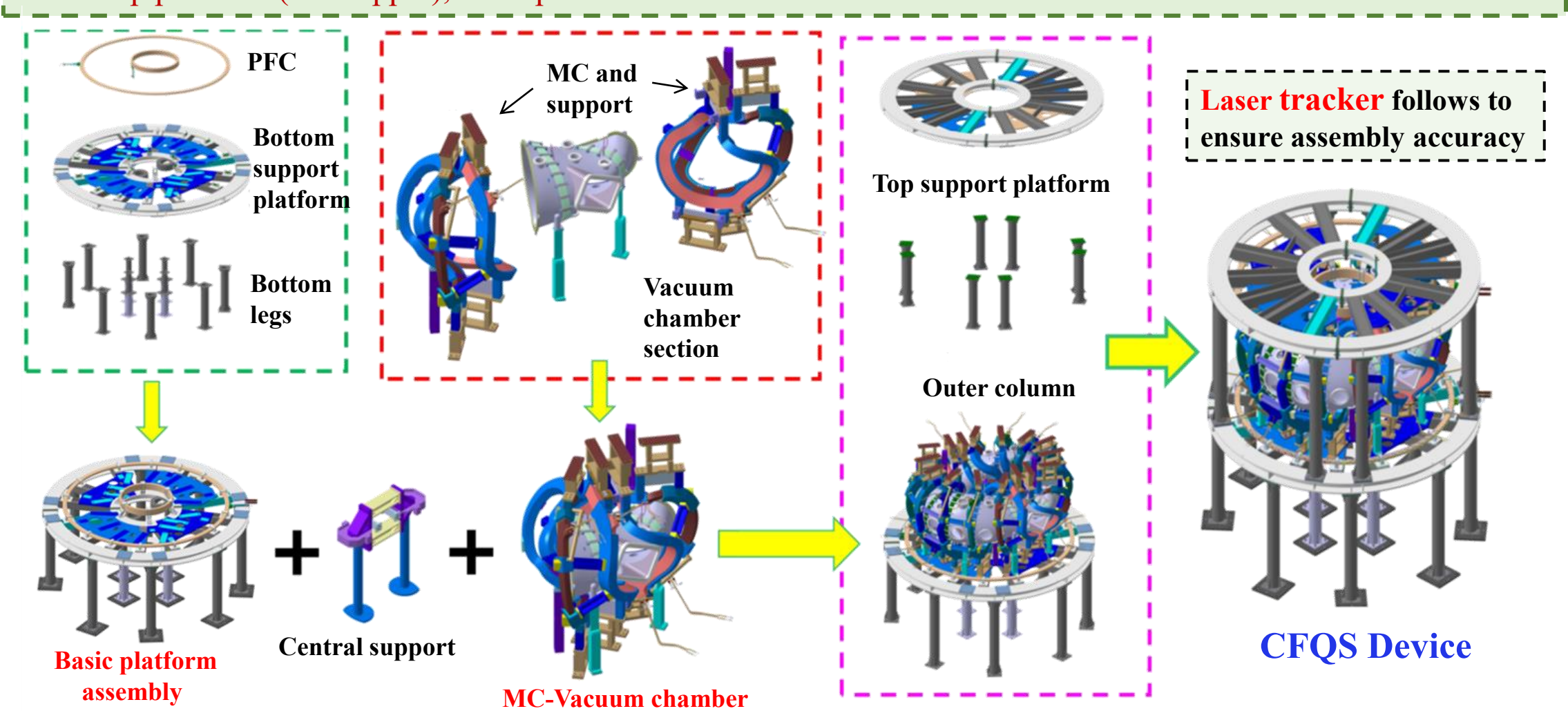


- Vacuum vessel: two type A and two type B; 6 mm stainless steel plates;
- Type A: four pieces, type B: seven pieces; all the pieces for type A/B was formed by hot pressing method, and the max. deviation of each pieces is about 5 mm:
- Two type A/B VV has been welded, the maximum deviation is about 5 mm.

Assembly flow chart of the CFQS device

Assembly order:

- Basic platform assembly (PFC and bottom platform);
- MC-Vacuum chamber and the related support structure (required high accuracy);
- Top platform (PFC upper), outer pillars.



Assembling process

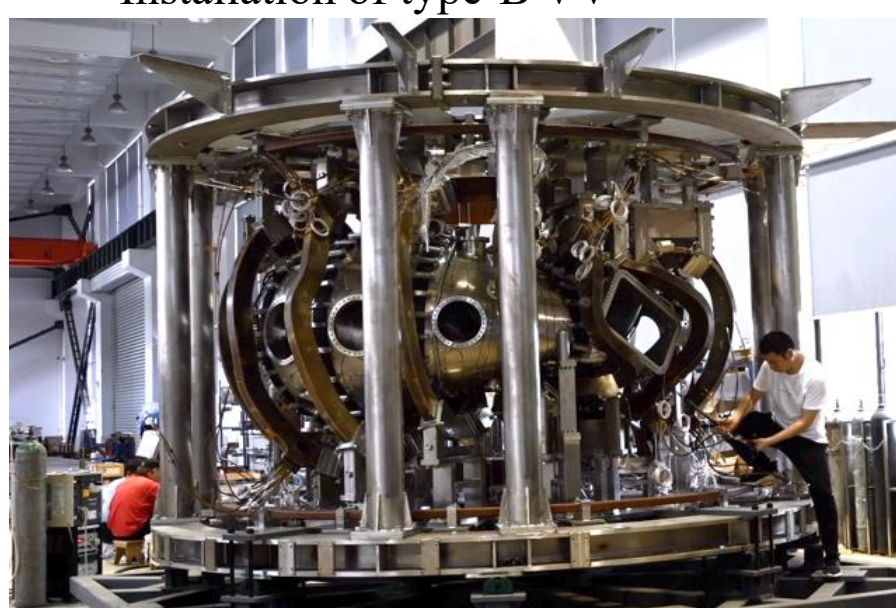
First MC installed on basic platform

2024.3.9



Installation of type-B VV

2024.6.26



Installation of MCs one by one

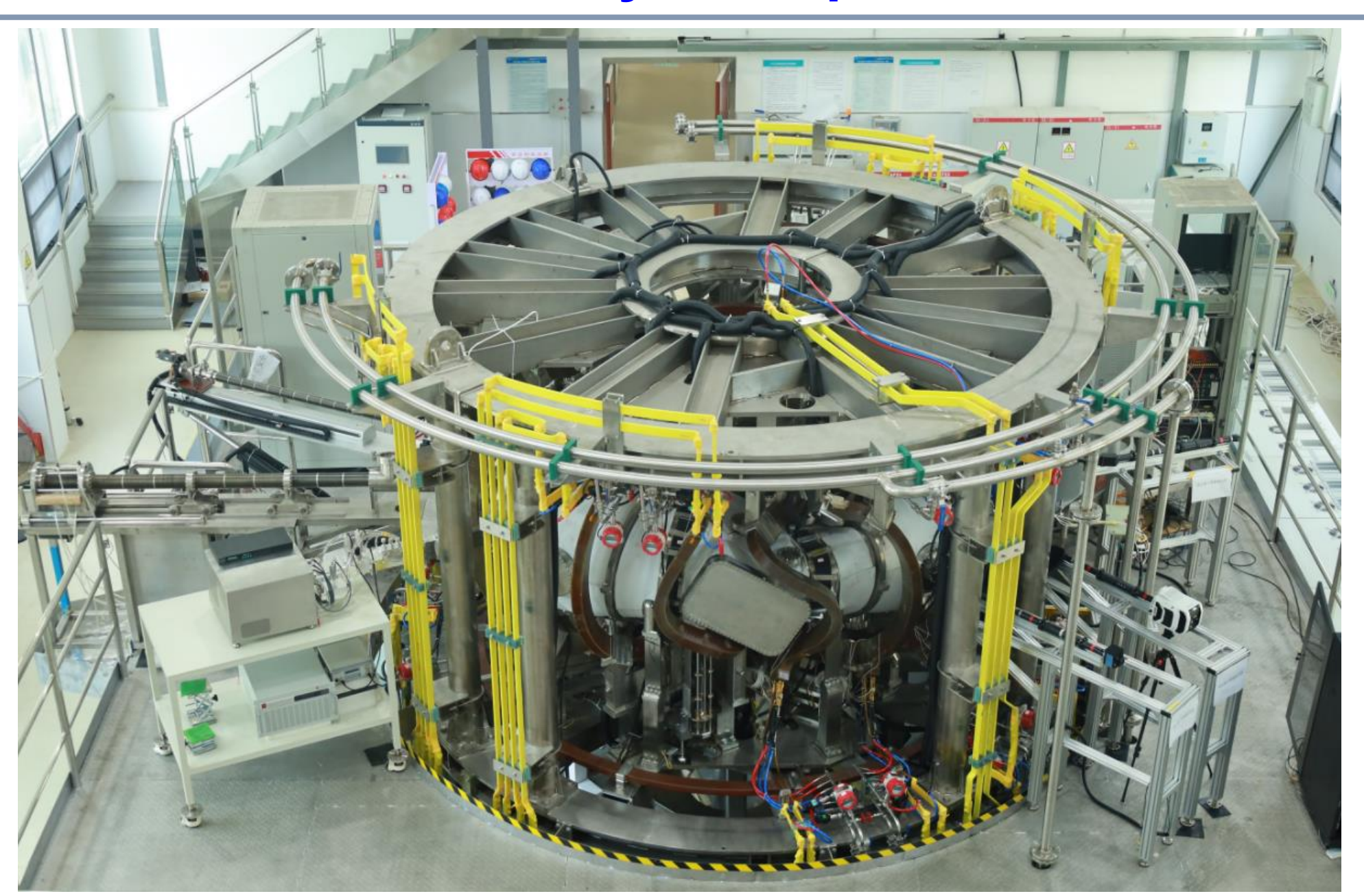
2024.4.29



Installation of water pipes



CFQS-T ready for experiment



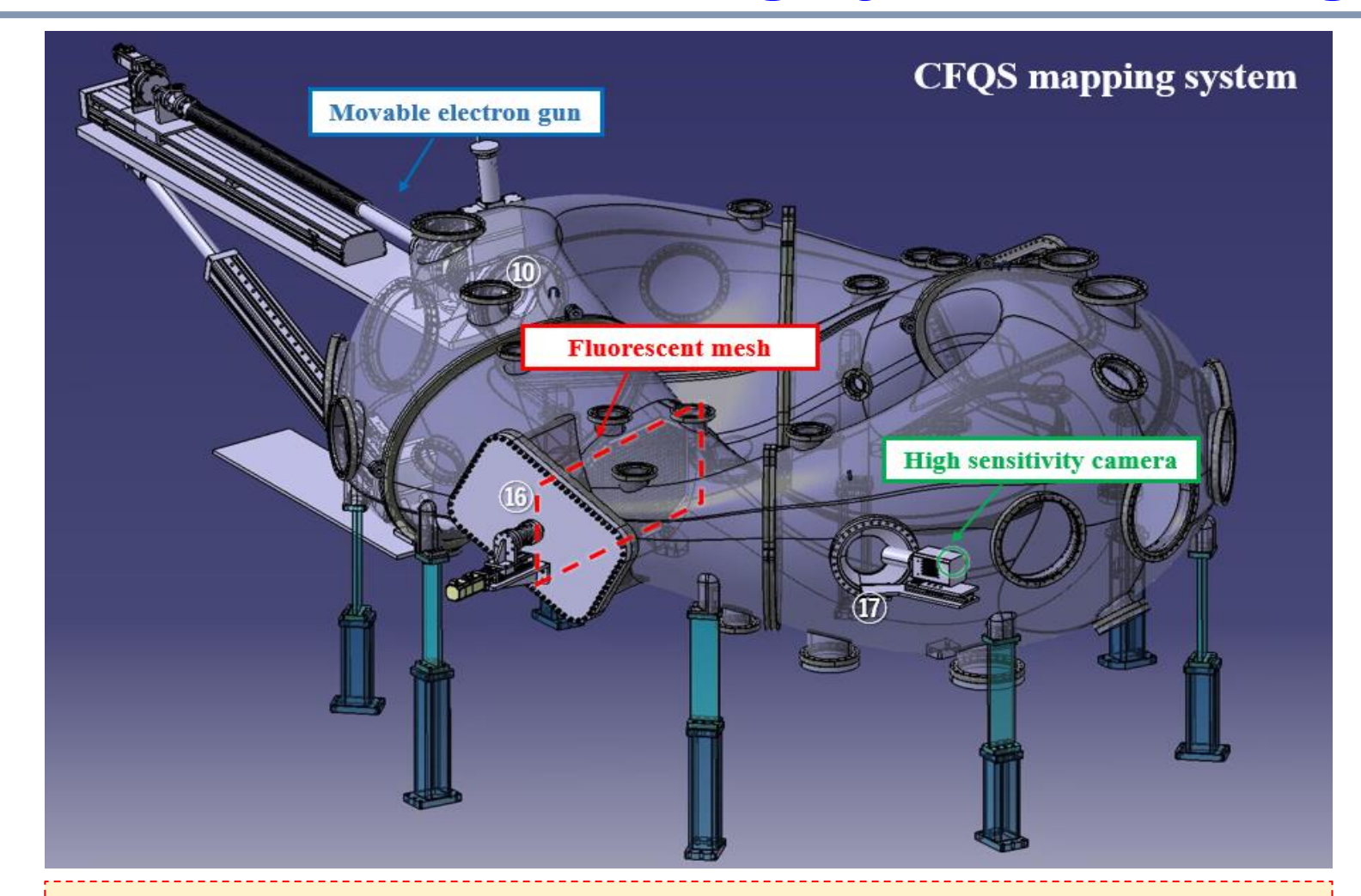


Outline



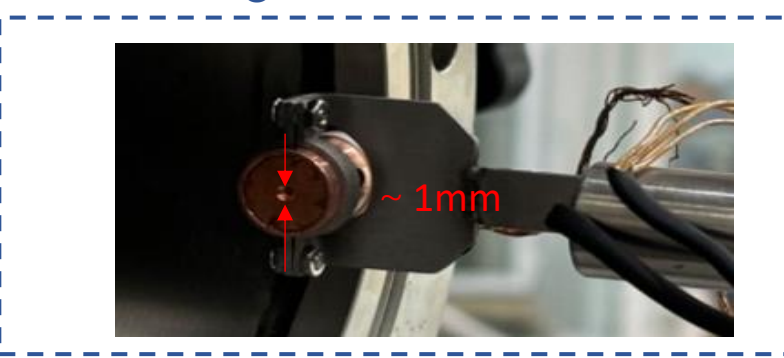
- Physical characteristics of CFQS
- Construction progress of CFQS
- Scientific achievements on CFQS-T
- Summary

Mapping system for magnetic field



It is mainly used to measure the three-dimensional magnetic field topology generated by the coil system and verify the accuracy of the quasi-axisymmetric magnetic configuration.

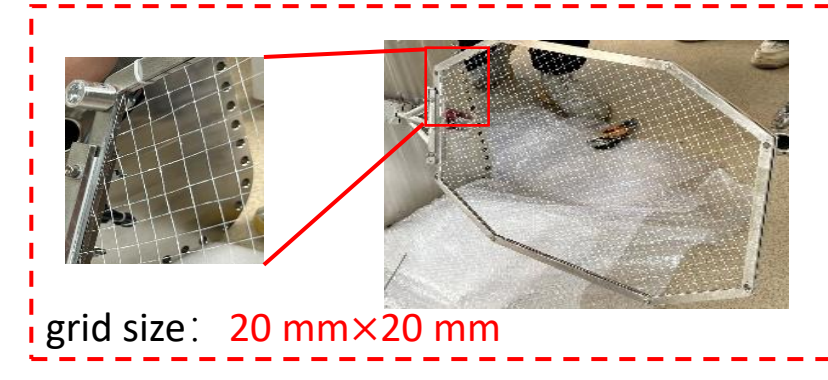
The electron gun



High sensitivity camera



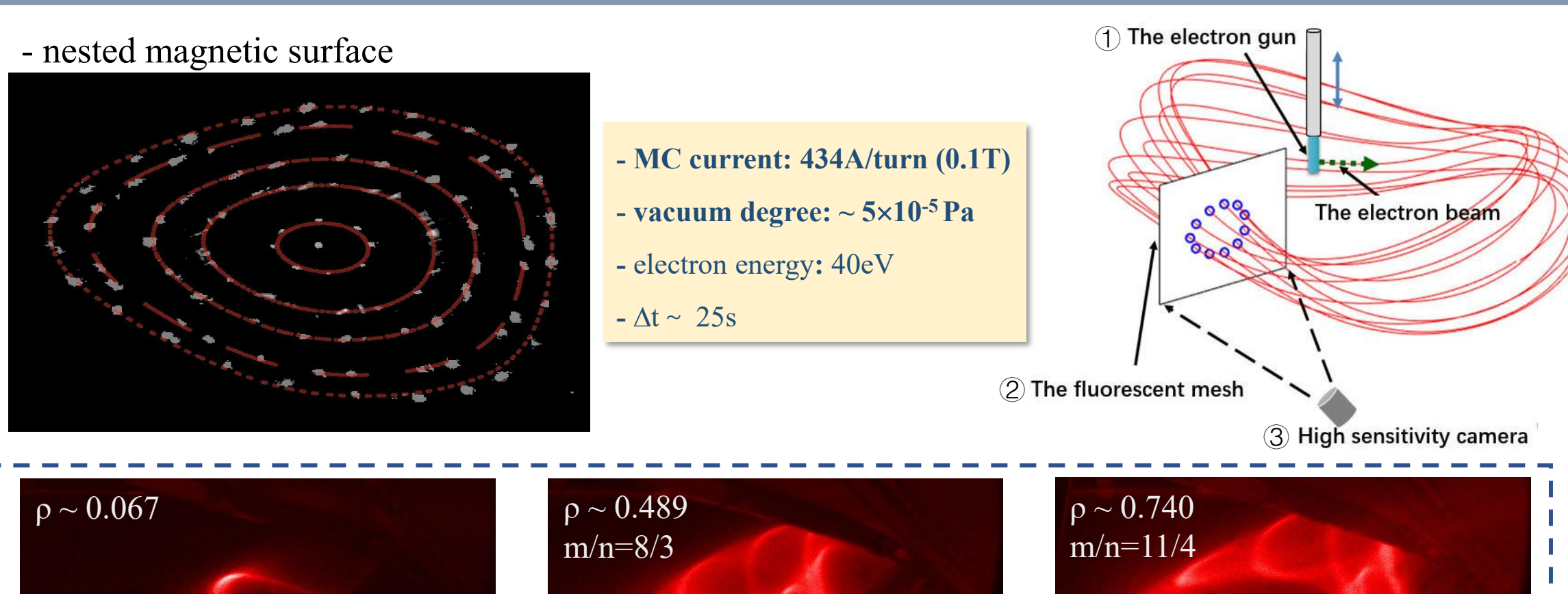
The fluorescent mesh

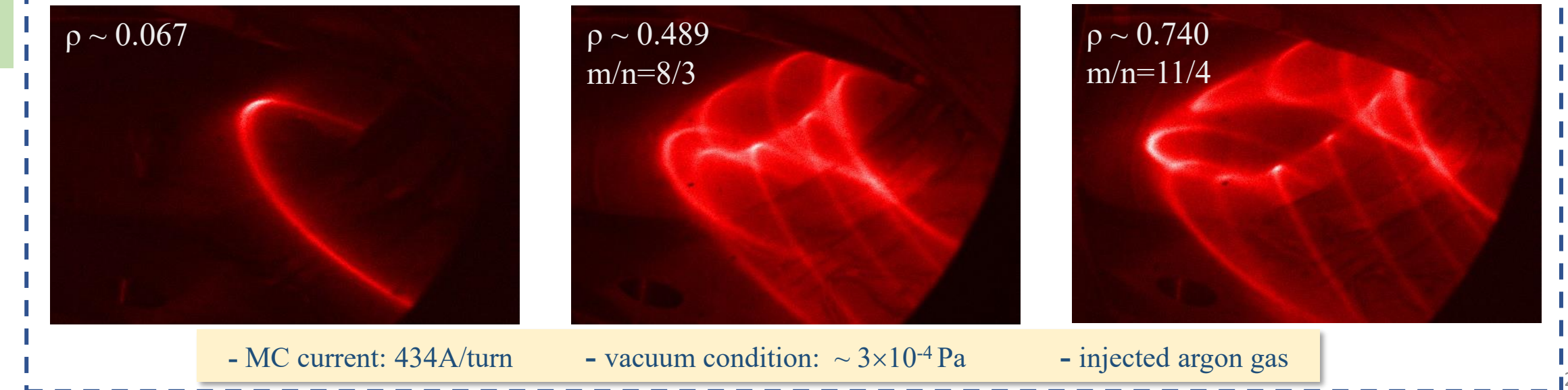


Validation of QA configuration

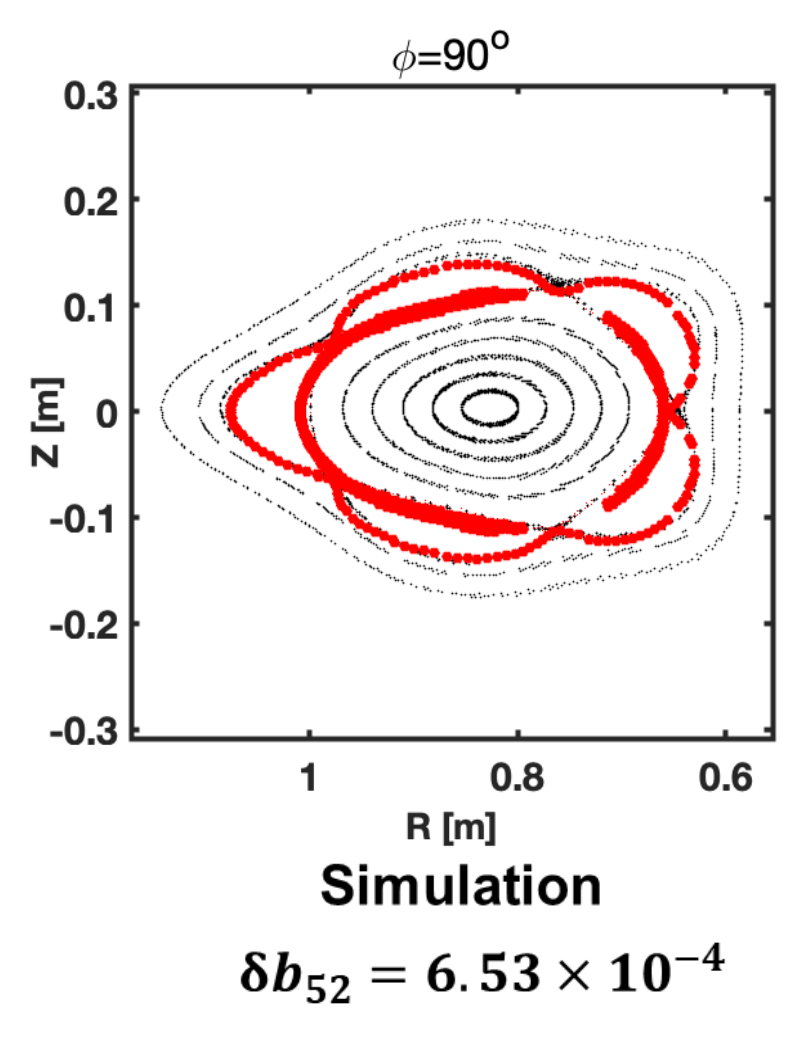
2D

3D

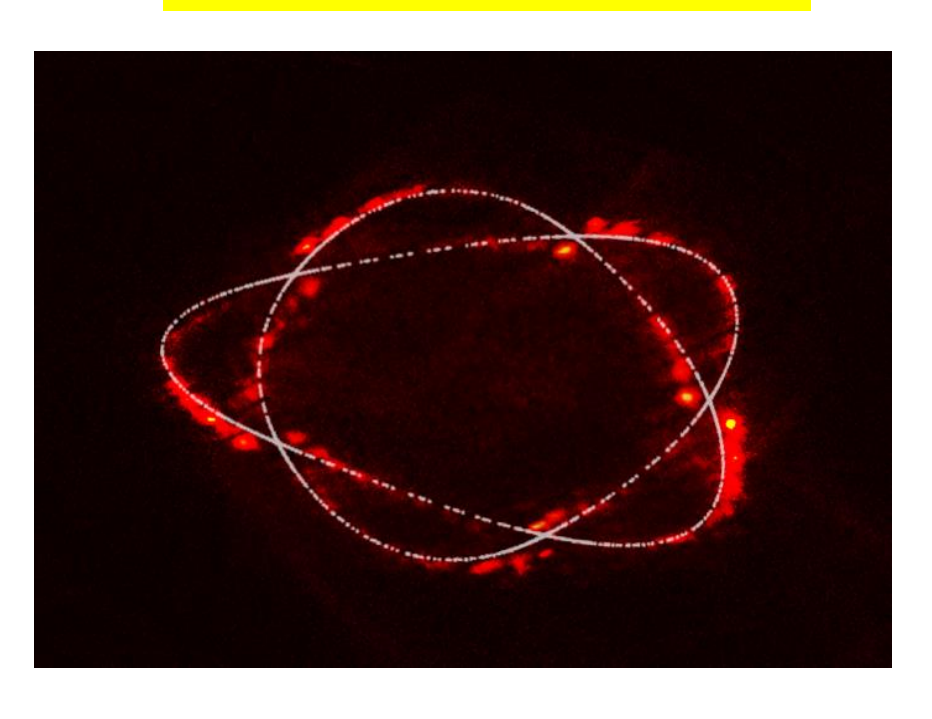




Error analysis of the magnetic topology



 δb_{52} generated by TF coils



Experiment

$$\delta b_{52} = 5.97 \times 10^{-4}$$

$$\frac{1}{2}(\psi - \psi_{mn})^2 + \delta \rho = Const$$

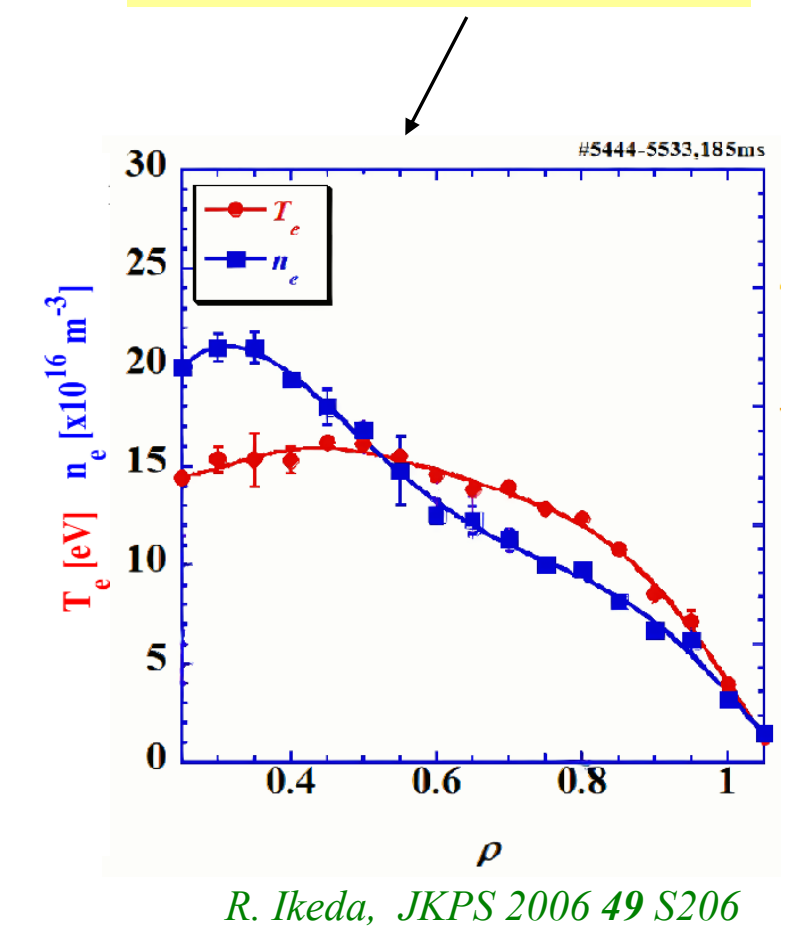
$$\delta \rho = \sum_{m,n} \frac{|\delta bmn|}{m\iota'} \cos(m\theta - n\zeta + \alpha_{mn})$$

Error field: $|\delta b_{52}(\exp) - \delta b_{52}(\sin)| = 5.6 \times 10^{-5}$

Comparison between CHS and CFQS-T

CHS (NIFS, Japan):

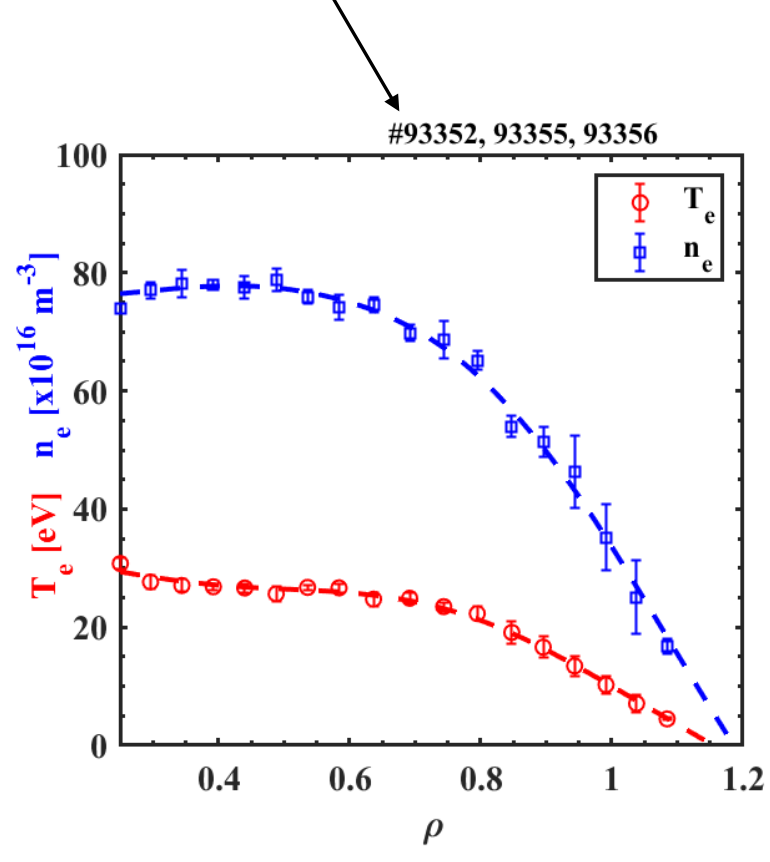
ECRH ~ 10 kW, 2.45 GHz B_t ~ 0.061 T, H plasma.

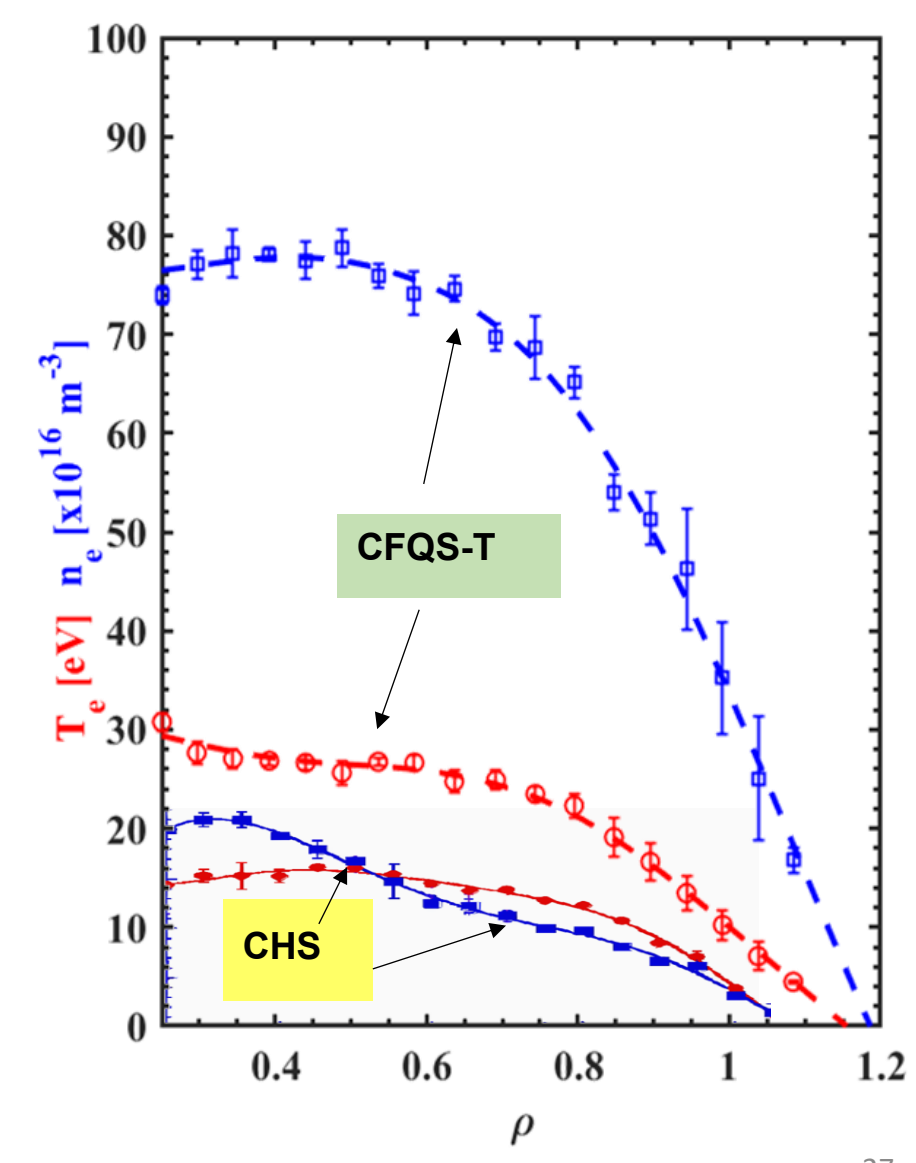


CFQS-T (SWJTU, China):

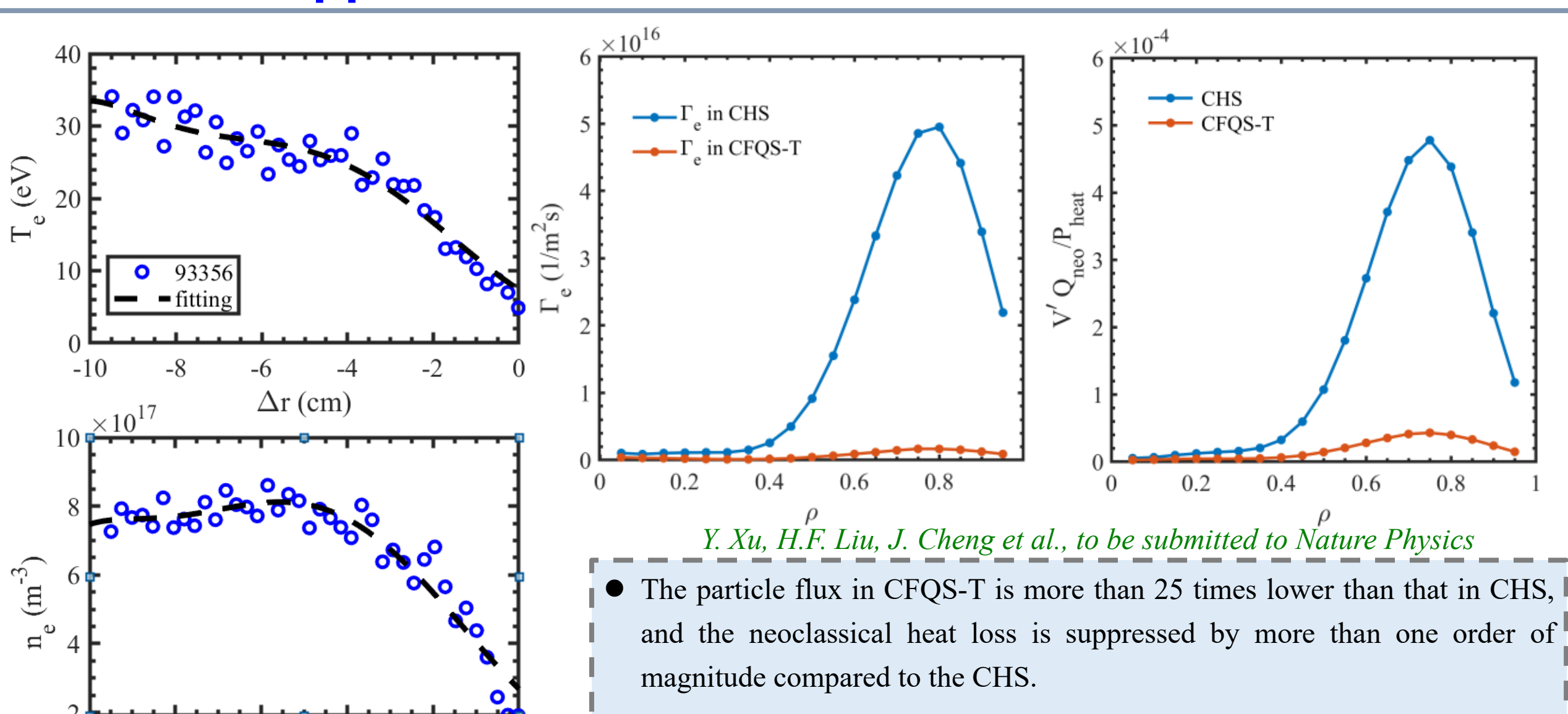
ECRH \sim 9 kW, 2.45 GHz.

Bt ~ 0.069 T, H plasma.





Suppression of neoclassical flux in CFQS-T



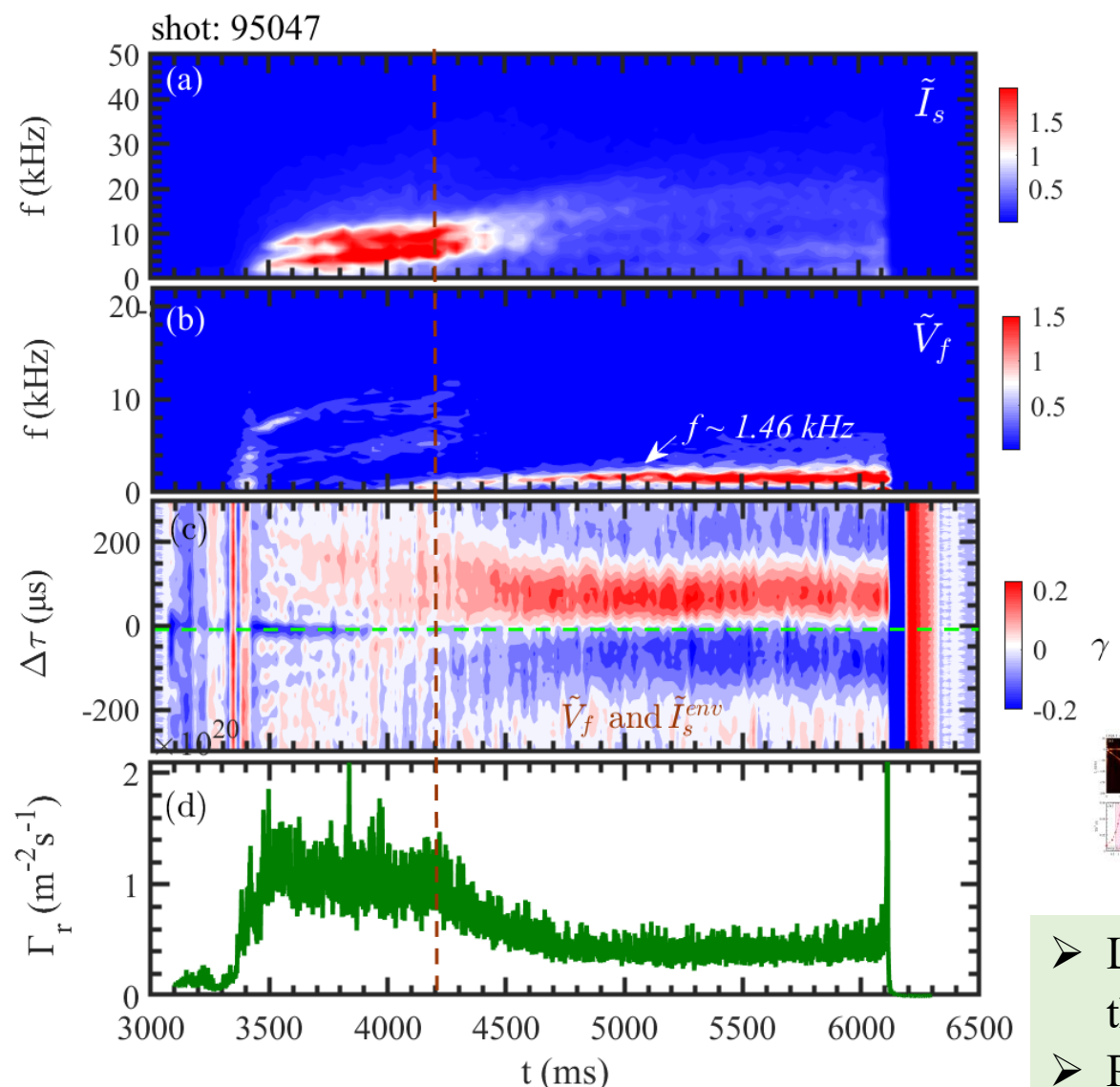
of # 93356. $E_r = 0$.

 Δr (cm)

 I_{MC} =327 A (Bt = 0.069T), use the electron temperature and density proflies

First observation of zonal flows in CFQS-T

Experimental parameters: H_2 discharge, P_{ECH} =3kW



X. Chen, J. Cheng, Y. Xu et al., to be submitted to PRL

- ➤ Low frequency zonal flow (LFZF) is spontaneously generated via three-wave nonlinear interaction;
- > Plasma confinement is improved by LFZF.



Outline



- Physical characteristics of CFQS
- Construction progress of CFQS
- Scientific achievements on CFQS-T
- Summary



Summary



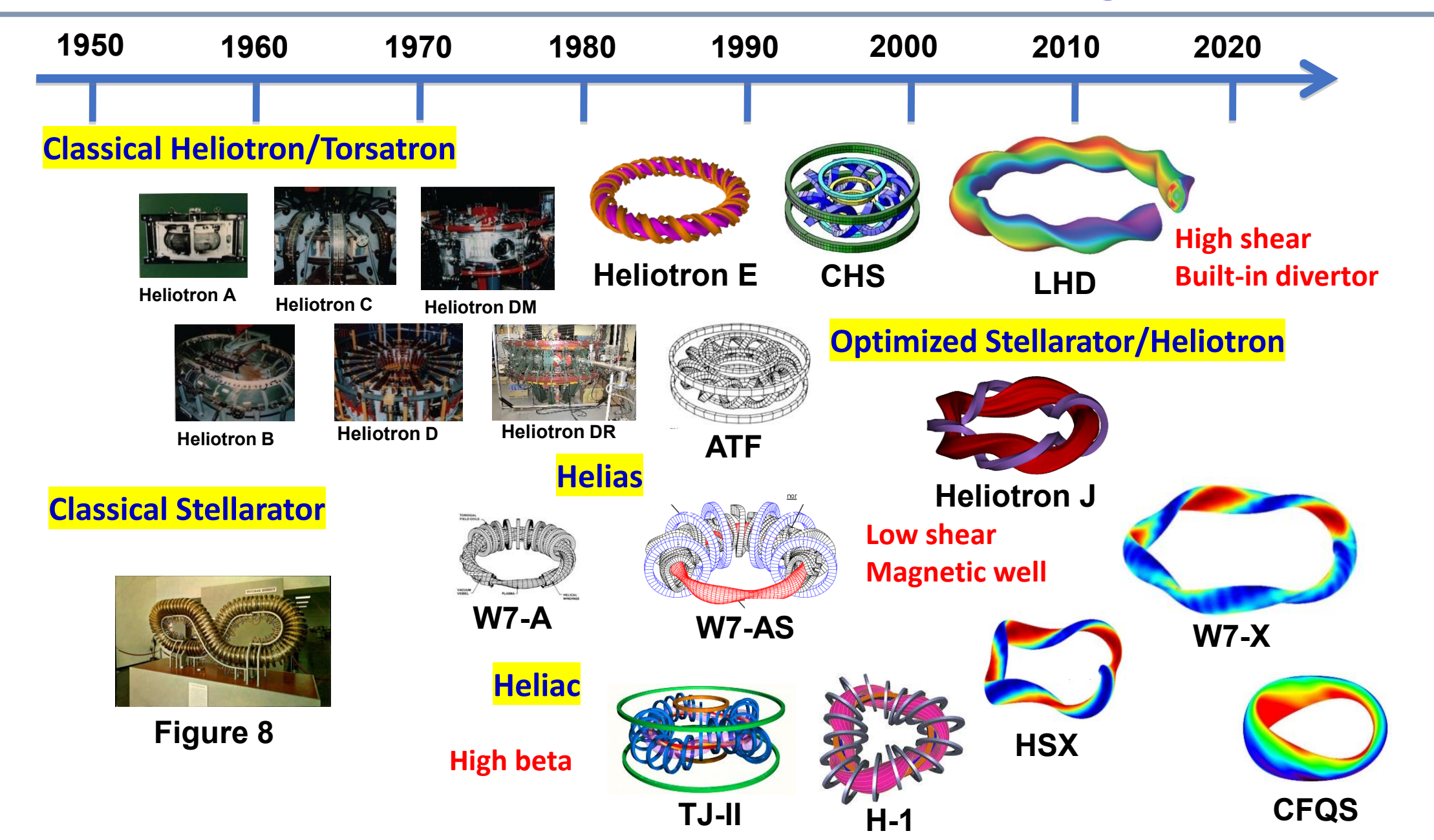
- CFQS Physics and Engineering Design Completed
- CFQS Construction Progresses Smoothly
- CFQS-T Has Achieved Preliminary Experimental

Results...



Thanks for your attention!

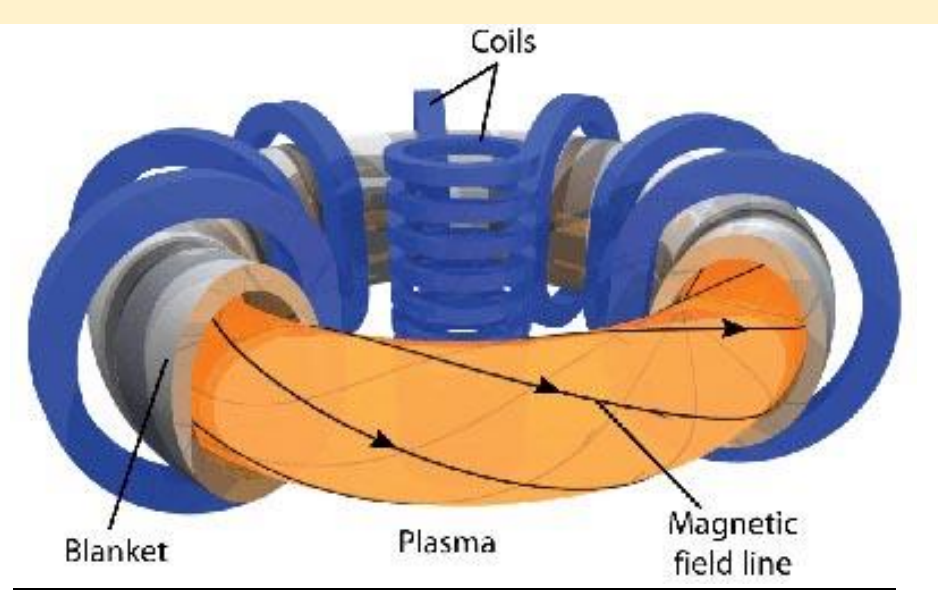
Optimization of stellarator configuration



Motivation of the joint CFQS project

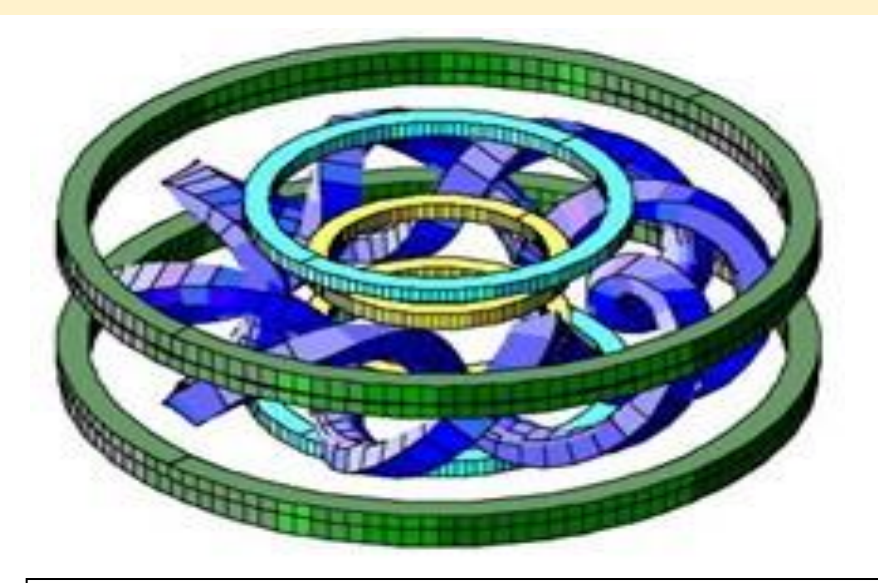
The Chinese First Quasi-axisymmetric Stellarator (CFQS):

- Jointly designed by SWJTU (China) and NIFS (Japan), and constructed by SWJTU.
- Main purpose is to verify the advantage of quasi-axisymmetric stellarator in reducing neoclassical transport for the first time in the world.



Tokamak (with I_p)

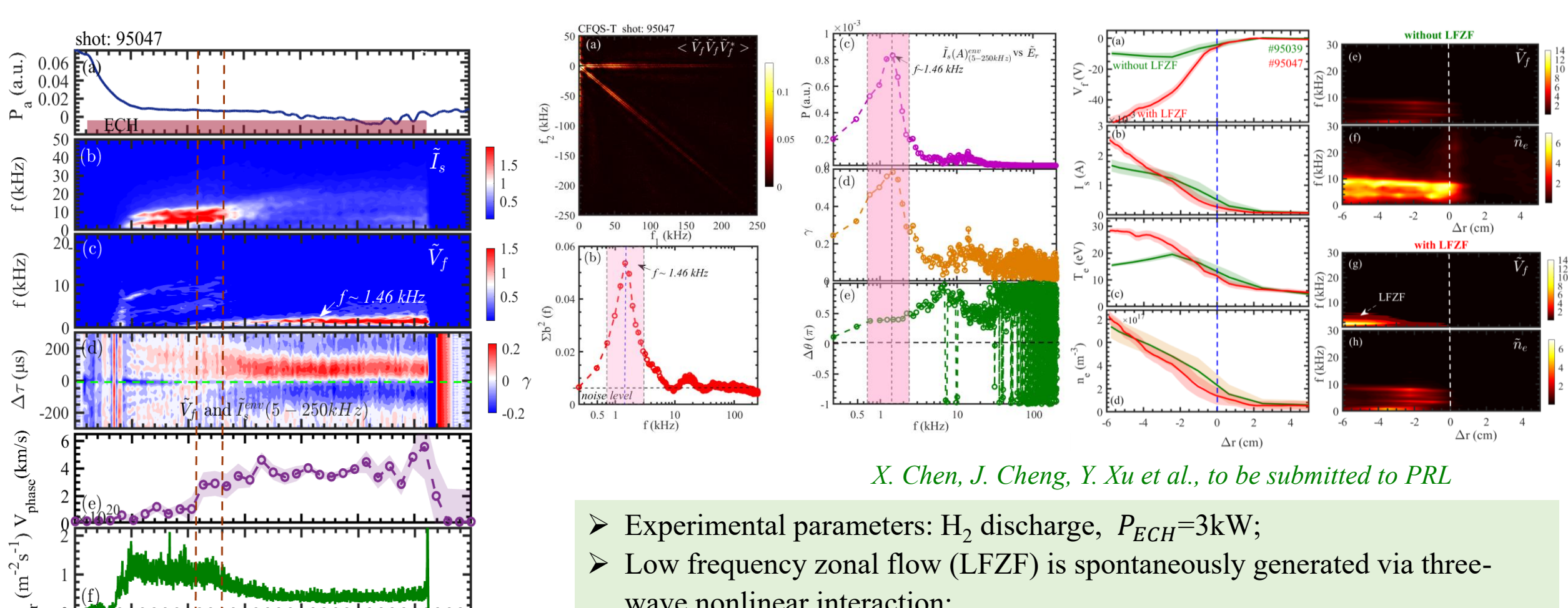
- Simple configuration
- low neoclassical transport
- Less freedom degrees
- More MHDs, Major disruption



Stellarator (without I_p)

- Steady-state operation
- less MHD, no major disruption
- **■** Technical complexity
- high neoclassical transport

First observation of zonal flows in CFQS-T



 $\begin{array}{ccc}
 & 0.08 & 0.00 \\
 & 0.06 & 0.00 \\
 & 0.02 & 0.00
\end{array}$

f (kHz)

t (ms)

- wave nonlinear interaction;
- ➤ The result clearly demonstrates that LFZF could modulate turbulence (5-30 kHz), consistent with theoretically-predicated predator-prey model;
- The turbulence suppression by LFZF is found to facilitate the steep of edge electron pressure profile.

Backup

